DESIGN AND FABRICATION OF A SIMPLE FOUR POINT PROBE SYSTEM FOR ELECTRICAL CHARACTERIZATION OF THIN FILMS

AGUMBA O. JOHN [B.Ed. (Sc.)]
I56/10400/2006

DEPARTMENT OF PHYSICS

A thesis submitted in partial fulfillment of the requirements for the award of the degree of Master of Science in the School of Pure and Applied Sciences of Kenyatta University

March, 2010

DECLARATION

This thesis is my original work and has not been presented for the award of a degree or any other award in any University

Signature Date

…….. ……

Agumba O. John

Department of Physics

Kenyatta University

This thesis has been submitted for examination with our approval as University Supervisors

Signature Date

…….. ……

Dr. Patrick M. Karimi

Department of Physics

Kenyatta University

Signature Date

…….. ……

Prof. John Okumu

Department Physics

Kenyatta University

Signature Date

…….. ……

Dr. Walter K. Njoroge

Department Physics

Kenyatta University

DEDICATION

This thesis is dedicated my friend and dear wife Martha and our dear son Ron Mishael.

ACKNOWLEDGEMENTS

Foremost, I would like to sincerely thank my thesis advisors; Dr. Patrick M. Karimi, Prof. John Okumu and Dr. Walter K. Njoroge for their able guidance and support during my research periods and helping me reach the research objectives with strong motivation and dedication. Special thanks goes to Dr. Patrick M. Karimi who introduced me to LabVIEW, an amazing piece of software which I have used almost everywhere in all my research work. A lot of thanks goes to the chairman Physics department, Kenyatta University Dr. Charles Migwi for being supportive throughout this work. Not to forget is Prof. I.V.S. Rathore, the chairman D.B.P.S, Physics department for his guidance during the thesis writing.

This project involved a lot of lab work, and a lot of custom-built equipment. I am very grateful to all the Physics department technical staff led by Mr. Simon Njuguna who made things for me, lent me apparatus, and generally did things that were beyond the call of duty. Not to forget is Mr. Muthoka, chief technician, solid state laboratories, University of Nairobi, who made some laboratory equipment available to me.
I was blessed to be surrounded by excellent colleagues: Okiambe, Mugambi, Jobunga, Kebwaro, Gesuka, Karanja, Wekunda, Mukeke, Obanda, Zavani, Omayio, Mugwanga and Ochillo. I want to register my gratitude for your support during this research period.

To my parents: Thank you for your unconditional love and support. In your demise, dad, you are my supreme role model and the embodiment of integrity, courage, and honor. Mom, thanks for your undying kindness and care. You are the anchor that has kept our family going in the absence of our dad. To my uncle Johnson Oluoko, you have been unchallengeable pride for me. Thanks for introducing the culture of academia to our family of Kondiek. If I am lucky, I will someday be half the extraordinary person you have become and meet your dreams.

Finally, I would like to thank my dear wife, Martha and our junior Ron, who have been a source of unlimited love, friendship, laughter, support and motivation.

Above all I want to thank the Almighty God who has taken me this far. I confess that the strides I have made were only possible because He was my strength and motivator. Oh! Dear Lord! I can say “I am nothing without You” All the glory and honor goes back to You.

TABLE OF CONTENTS

CHAPTER 3
THEORETICAL BACKGROUND

CHAPTER 4
MATERIALS AND METHODS

LIST OF TABLES

LIST OF FIGURES

LIST OF ABBREVIATIONS

APCVD	Atmospheric Pressure Chemical Vapor Deposition
API	Application Programming Interface
BEC	Bose-Einstein Condensation
BIOS	Basic Input / Output System
COM	Communication
CVD	Chemical Vapor Deposition
DB	Data Bus
DCV	Direct Current Voltage
DUT	Device Under Test
ECP	Extended Capability Port
EPP	Enhanced Parallel Port
GND	Ground
GPIB	General Purpose Interface Bus
GUI	Graphical User Interface
IEEE	Institute of Electrical and Electronic Engineers
IRQ	Interrupt Request
LabVIEW	Laboratory Virtual Instruments Engineering Workshop
LED	Light Emitting Diode
LPCVD	Low Pressure Chemical Vapor Deposition
LPT	Line Printing Terminal
MOCVD	Metal Oxide Chemical Vapor Deposition

NPLC	Number of Power Line Cycles
OS	Operating System
PC	Personal Computer
PCI	Peripheral Component Interconnect
PECVD	Plasma Enhanced Chemical Vapor Deposition
PnP	Plug and Play
PVD	Physical Vapor Deposition
PXI	PCI eXtensions for Instrumentation
RF	Radio Frequency
RS	Recommended Standard
SCPI	Standard Commands for Programming Instruments
SMU	SourceMeter Unit
SPP	Standard Parallel Port
TTL	Transistor-Transistor-Logic
UART	Universal Asynchronous Receiver Transmitter
USB	Universal Serial Bus
VI	Virtual Instruments
VISA	Virtual Instruments Software Architecture
VISAIC	Virtual Instruments Software Architecture Interactive Control
VPE	Vapor Phase Epitaxy
VXI	VME eXtensions for Instrumentation
XRD	X-Ray Diffraction

ABSTRACT

The electrical characteristics of semiconductor thin films are of great practical interest in microelectronics industry hence the need to measure these parameters in a cheaper and faster manner possible. This study has embarked on design and fabrication of a simple, effective and portable computer-aided four point probe system for thin film sheet resistivity measurement. A four point probe head has been designed and fabricated from easily available materials. A relay switching device has also been designed and fabricated to perform switching of the probe tips on the sample surface as per the Van der Pauw set up. A Keithley SourceMeter 2400 model has been interfaced to a LabVIEW running computer via the serial port (RS-232 port) for its full control by the computer. The relay switching device has also been interfaced to the computer via the printer port (LPT1 port). The fabricated probe head, the relay switching device and Keithley SourceMeter were used to probe the samples as per the Van der Pauw set up with a square symmetry adopted for sheet resistivity measurement. To test the workability and reliability of the fabricated system for thin film sheet resistivity measurement, the sheet resistivity of Cu_2O semiconductor thin films prepared by DC reactive magnetron sputtering technique were measured. The sheet resistivity measured at room temperature of 23 ^oC was found to be 55.65 Ω cm. However, as the samples were exposed to temperature rise, the sheet resistivity was found to decrease and was at its minimum value of 29.67 Ω cm at 170 ^oC. Cu_2O thin films prepared at different sputtering pressures were also electrically characterized using the system. The sheet resistivity of the thin films were found to increase with increase in sputtering pressure. Films deposited at sputtering pressure of $1.8x10^{-2}$ mbar had sheet resistivity of 33.63 Ω cm and this increased to 62.23 Ω cm for films prepared at higher sputtering pressure of $2.4x10^{-2}$ mbar. From the measurements obtained, it was found from the study that the system offers a reliable, effective and simple technique for thin film sheet resistivity measurements.

CHAPTER 1

INTRODUCTION

1.1 Background to the Study

Various methods have been used in the laboratory for measurements of a number of physically measurable parameters. This has mainly been done by manual handling of traditional analogue devices (Owade, 1998). However, today there is a fundamental trend in automated test and measurement industry that has had a heavy shift towards software-based test and measurement systems. Laboratory automation involves controlling laboratory equipment remotely by using a controller like computer in order to achieve laboratory measurements. For this control, there is need for communication between computers and peripheral devices (interfacing) achieved by use of industry standard stand-alone buses such as serial (RS-232, RS-422 or RS-485), parallel (LPT port), GPIB, Ethernet, IEEE 1394 (FireWire) and wireless communication such as Bluetooth. Also, modular buses such as PCI, PXI, PCI Express and VXI are used for interfacing. Computer-aided tests and measurements improve the speed of the laboratory measurements, their precision and the reliability.

Thin film semiconductors play a crucial role in hi tech industries with major exploitation in microelectronics, communication and optoelectronics (Ohring, 1992). Cu_2O thin films being semiconductors offers a wide range of promising applications such as low cost photovoltaic cell fabrication due to their high absorption coefficient in the visible range of 0.35-0.80 μm and low band gap of 2.00 eV. Their other application areas include use in electro-chromic coatings, catalytic applications and in high-T_c superconductors. This

semiconductor thin film has attracted attention for many years due to its cuprite structure, its connection with Bose-Einstein Condensation (BEC) of excitons, its stoichiometric deviations arising from preparation methods and parameters, ease of preparation, non-toxic nature and abundance (Sivasankar *et al.,* 2008). Nevertheless, the progress of its application has been limited by difficulties associated with preparation of high quality films since many of its preparation methods results in co-deposition of phases of Cu, Cu_2O and CuO (Balamurugan and Mehta, 2001).

Thin film sheet resistivity which is a surface inherent resistance to flow of current determines the surface impurity content hence doping level and electron mobility (Maria *et al*., 2002). This in turn affects its component's capacitance, the series resistance and threshold voltage. For this reason, surface resistivities are measured throughout wafer fabrication process to ensure proper doping as well as to monitor the effect of thermal cycling on dopant redistribution (Smits, 1958). The knowledge of sheet resistivity of semiconductor thin films and of Cu_2O in particular is of great practical importance for the fabrication of electronic components such as rectifier diodes, transistors, photovoltaic cells and humidity sensors since this parameter affects their performance in these applications (Sze, 1981). There is hence the need to measure this parameter in an easy, faster and accurate manner possible. However, the measurement of thin film sheet resistivity like any other parameter being of no exception has mainly been done either by the old manual methods or by use of two point probe method which inadvertently introduces errors due to probe resistance, spreading resistance and contact resistance between probing tips and the samples (Schroeder,1998). Also, commercial probing

devices which are expensive and not easily available have been used. Furthermore, programming languages such as C, C++, C#, FORTRAN, JAVA, Delphi and Matlab among others which have mainly been used for programming most of the laboratory devices for thin film sheet resistivity measurements being text based languages have long statements that are cumbersome to develop, write and debug. Due to the above limitations, the precision and accuracy of the results obtained coupled with the time taken for these measurements are in most cases compromised. As opposed to the above textual languages, LabVIEW graphical language is preferred for programming the laboratory sheet resistivity measurement instruments for data acquisition and interfacing. Being a graphical language, it is interactive, simpler and easier to develop (Rick *et al.,* 2001).

This study has designed and fabricated an inexpensive, simpler and faster software-based technique for electrical characterization of thin film samples and for proof of the system's workability and reliability, sheet resistivity of Cu_2O semiconductor thin films prepared at different sputtering conditions have been measured. The dependence of the sample's sheet resistivity on temperature variation and a possible deviation in the crystal lattice of the Cu_2O thin films that may arise from sample's temperature change has also been studied. With the results obtained compared to the theoretical and available experimental results, the reliability of the developed system has been tested.

1.2 LabVIEW Programming Language

Developed by National Instruments in 1986, LabVIEW is a programming language that depicts program code graphically rather than textually (Higa and Lord, 2002). One major benefit of using LabVIEW programming language as used in this study rather than text-based languages such as VB, C, C++, C#, FORTRAN, JAVA, Delphi and Matlab among others is that the program codes are written by simply connecting icons. In addition, the graphical programming languages offer the performance and flexibility of text-based programming languages, but conceal many programming intricacies such as memory allocation and syntax. The language involves structured dataflow diagramming (Jeffrey and Jim, 2006). Because it is the flow of data between objects on a block diagram and not sequential lines of text that determines execution order in LabVIEW, one can create diagrams that simultaneously execute multiple operations (National Instruments, 1998). Consequently, LabVIEW is a multitasking system capable of concurrently running multiple execution threads and multiple VIs. LabVIEW accelerates development over traditional textual programming by a significant factor and most importantly, it has many interesting features that make it a very useful tool for device interfacing, data acquisition, data manipulation and data presentation which are core areas of this study (Pogula, 2005).

1.3 Statement of the Research Problem

In this study, a simple and portable four point probe system has been designed and fabricated. For proof of its workability, the system has been used for electrical characterization of Cu_xO_y semiconductor thin films and more particularly Cu_2O prepared

at different sputtering pressures using DC magnetron sputtering technique. The effect of temperature variation on the sheet resistivity of the thin films has also been investigated. This system has been found to offer a reliable solution for electrical characterization of thin films deposited at different sputter conditions and films exposed to different temperatures.

1.4 Objectives of the Research Study

The main objective of this research study is to design and fabricate a simple, portable and software-based laboratory four point probe system required for conducting electrical characterization of thin film sheets and for proof of the system's workability, sheet resistivity of Cu_2O semiconductor thin films deposited at different sputter conditions and films exposed to various temperatures are measured. The specific objectives are:

(i) To design and fabricate a probe head from easily obtainable materials

(ii) To design and fabricate a switching device to perform switching of probe tips on the thin film sample's surface as per Van der Pauw set-up

(iii) To develop LabVIEW VIs for full control of Keithley SourceMeter apparatus by the computer and for data transfer between the computer and the apparatus via serial port (RS-232 port)

(iv) To develop a labVIEW VI for interfacing the fabricated Van der Pauw switching device to a computer via the parallel port (Printer port)

(v) To deposit Cu_2O thin films on glass substrates at various sputtering pressures by means of DC reactive magnetron sputtering technique using Edward's 306 AUTO vacuum deposition unit

(vi) To measure the sheet resistivities of the Cu_2O thin films deposited at different sputtering pressures using the fabricated system and to compare the results obtained with the theoretical and available experimental values to prove its reliability

(vii) To investigate the effect of thermal cycling on the sheet resistivities of the deposited Cu_2O thin film samples using the fabricated system

1.5 Rationale of the Research Study

Sheet resistivities of thin films and in particular, semiconductor sheets are very useful in microelectronics technologies hence it is necessary to measure these properties in a simple, cheap and faster manner possible. The commercial probing devices used for these measurements are expensive and not easily obtainable. Furthermore, most of them are manual and not user friendly hence the need to design and build a cheaper and easier to use computer-aided probing device. This study provides an interactive and simple interface system and data transfer between the SourceMeter apparatus, the switching device and a computer by use of LabVIEW VISA VIs. The system measures, displays and analyzes the I-V characteristics of thin films and use these parameters for sheet resistivity computation. Some of the merits derivable from this study include:

(i) Easy sample probing as per Van der Pauw set-up since the probing system is computer-aided as it is achieved by transistor operated relay switch controlled by a computer via its printer port. The probe head is also cheaper and simpler to operate as compared to commercial ones.

(ii) Easy and interactive data acquisition LabVIEW VIs for data transfer from Keithley SourceMeter to a computer via serial port using VISA VIs.

(iii) The VIs for the device interface, device control, data acquisition, data control, data analysis and data presentation are cheap and simple since a LabVIEW graphical programming is used as opposed to long text programs in text-based programming languages.

CHAPTER 2

LITERATURE REVIEW

2.1 Introduction

The electrical properties of thin films are determined by their chemical composition, the content and type of impurities in the thin film or on its surface, crystal structure of the thin film and the types and density of structural defects (Ogwu *et al*., 2007). In addition, as the applications of thin films extend to microelectronics, optoelectronics, magnetism and other areas, their electrical, optical and magnetic properties also have to be monitored and optimized. Four point probe technique has been a widespread method for electrical characterization of thin films for many years. This chapter presents research studies that have been performed on four point probe technique as per the Van der Pauw set -up. The studies that have been performed on electrical characterization of thin films and in particular, Cu_2O semiconductor thin films are also presented.

2.2 Four Point Probe Technique

The four point probe technique dates back to 1916 when Wenner used it to measure the earth's resistivity (Wenner, 1916). In 1954, Valdes adopted it for semiconductor wafer resistivity measurement (Valdes, 1954). Today, it is widely used in the semiconductor industry to monitor production process (Smits, 1958). The four point probe technique can be used to measure film thickness, but it is usually used to measure the sheet resistance of shallow layers (as a result of epitaxy, ion-implant, diffusion, evaporation or sputtering) and the bulk resistivity of bare wafers. Numerous investigations have been made on the

four point probe technique and measurement of sheet resistivity of thin films which are of great relevance to this study. Van der Pauw (1958) in a study on the method of measuring specific resistivity and Hall Effect of a disc of an arbitrary shape developed and presented a relationship between sheet resistance *(R_s)*, sheet symmetry factor *(F)*, correction factor *(Q)*, current *(I)*, voltage drop *(V)* and the film thickness *t* in SI units as shown in the equation below.

$$R_s = \frac{\pi}{\ln 2} F(Q) \left(\frac{V}{I}\right)_{Average} \Omega/Square \qquad (2.1)$$

This study showed that the correction factor (*Q*) depends on the sheet symmetry factor (*F*) by equation 2.2.

$$\frac{Q-1}{Q+1} = \frac{F}{0.693} ar\cosh\left(\frac{e^{0.693/F}}{2}\right) \qquad (2.2)$$

Halperin (1996) studied difference in significance between surface resistance and surface resistivity of a thin film using four point probe set-up. From this study, it was realized that surface resistance has no scientific significance as opposed to sheet resistivity since the former only depicts resistance between the opposite sides of a square. The sheet resistivity was found to affect the electron mobility on the film surface. However, this study did not look at factors that influence the sheet resistivity of thin film samples.

Owade (1998) in a study to design and develop a programmable laboratory interface systems for use in resistivity measurements designed a four point probe system for sheet resistivity measurement. Commercial probe head being expensive and not available in the

laboratory was designed and fabricated from easily available materials. However, ammeters and voltmeters were used to perform current and voltage measurements as opposed to SourceMeter unit as used in this study. Since assembly language for 8085 microprocessor was used to program this system, this involved long statements which were hard to write and debug. Furthermore, the sheet resistivity computations using the current and voltage readings were done manually.

Bautista (2004) performed a thin film sheet resistivity measurement where a collinear symmetry was adopted as shown in figure 2.1.

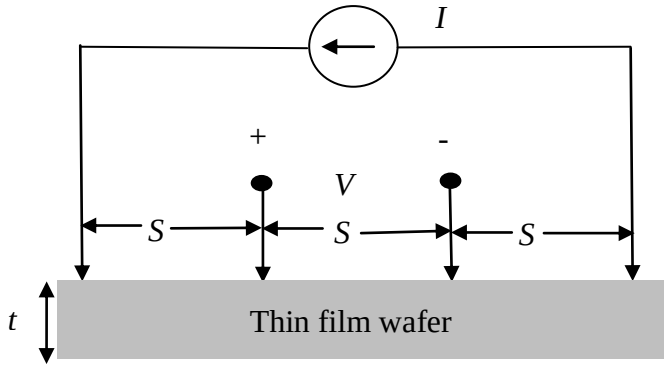

Fig. 2.1: A schematic of collinear four point probe method

where S is probe spacing, V is voltage drop across the sample, I is current in the sample and t is the film thickness. The theory behind this work was that a fixed current was injected into the wafer through the two outer probes, and a voltage measured between the two inner probes. In this study, Keithley SourceMeter 2400 was used to source current through the outer probes and voltage drop across the inner probes measured. From the

voltage and current readings obtained, surface resistance was computed. The study found out that sheet resistance can be given by equation 2.3.

$$R_s = 4.532\frac{V}{I} \tag{2.3}$$

from which sheet resistivity was computed. If probes with uniform spacing *S* were placed on an infinite slab material, then the sheet resistivity, ρ_s, was given in this study as:

$$\rho_s = \frac{\pi}{\ln 2} \times \frac{V}{I} \times t \times k \tag{2.4}$$

where *V* is the voltage drop across the surface sample, *I* is sourced current, *t* is the film thickness and *k* is the correction factor. In this study, it was realized that the probes tips should be able to make ohmic contact with the thin film sample. The SourceMeter unit was however manually used and programmed using text based configuration and data acquisition remote language which required great mastery of the SCPI commands.

2.3 Electrical Characterization of Thin Films

The method of film preparation has been found to be the main factor affecting the electrical properties of thin films as it determines the film crystal perfections, structural and electronic defect concentration, dislocation density, void or porosity content, grain morphology, chemical composition and stoichiometry and electron trap densities. This section presents studies that have been performed on the effect of deposition parameters on sheet resistivities of Cu_2O thin films. The studies on effects of temperature variation on the sheet resistivities of Cu_2O thin films are also outlined in this section.

Toney *et al*. (2003) studied the effect of amount of oxygen flow into a sputter chamber during Cu_2O DC reactive sputter deposition and found out that it affects sheet resistivity. The study showed that there is a sharp decrease in resistivity of the thin films with increase in oxygen flow into the chamber due to reduction of Cu/Cu_2O interface roughness. This also suggested increase in the crystal crystallinity of the film formed.

Reddy *et al.* (2005) carried out a study on the influence of substrate bias voltage on the properties of DC reactive magnetron sputtered Cu_2O films. The effects of the substrate bias voltage on structural, electrical and optical properties were systematically analyzed. With the other sputtering conditions maintained at fixed values, the bias voltage was increased from 0V to -80V. It was realized that the electrical resistivity of the films decreased from $4.6x10^1$ Ω cm to $1.0x10^1$ Ω cm with the increase of substrate bias voltage from 0 to -45 V and thereafter it increased to $1.6x10^1$ Ω cm at a higher bias voltage of -80 V as depicted in figure 2.2.

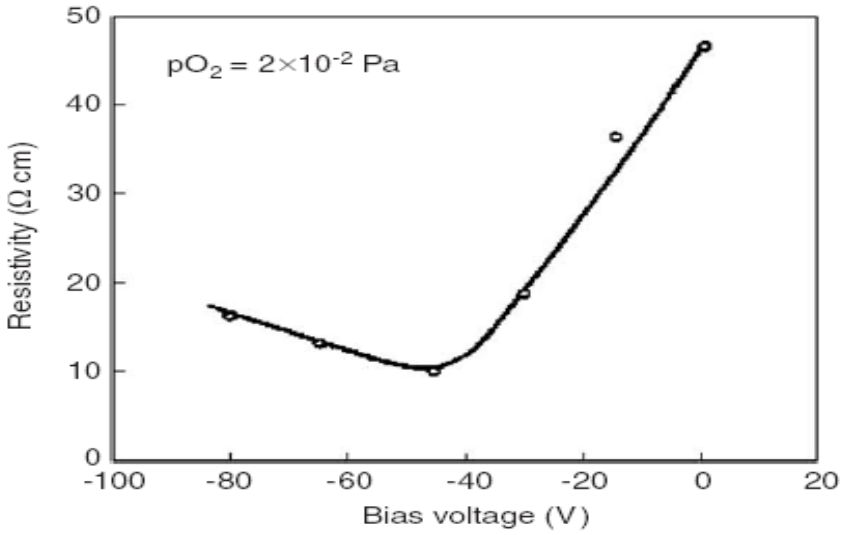

Fig. 2.2: Variation of electrical resistivity with substrate bias voltage (Reddy *et al.*, 2005).

Sivasankar *et al.* (2007) studied the effect of sputtering pressures on structural, optical and electrical properties of DC reactive magnetron sputtered Cu_2O thin films. In the study, four point probe method with linear symmetry adopted was used to measure thin film sheet resistivity. The electrical resistivity of the films was found to increase from 1.1 $x10^1$ Ω cm to 3.2 $x10^3$ Ω cm with increase in sputtering pressure from 1.5 Pa to 8.0 Pa.

Onimisi (2008) carried out a study on the effect on annealing on the resistivity of Cu_2O solar cells and realized that the resistivity is a function of the power output of such solar cells. Results revealed that the annealing of Cu_2O samples improves the cell's output performance as compared to that of unannealed samples by about 36%. With oxidation varied with temperature from 950 ^oC to 1050 ^oC, the resistivity varied from 501.04 Ω cm

to 498.14 Ω cm. Annealing was found to be a great factor in varying the electrical resistivity of the Cu_2O thin films.

Sivasankar *et al.* (2008) later studied the effect of sputtering power on electrical properties of DC reactive magnetron sputtered Cu_2O thin films. The films formed at low sputtering power of 0.38 Wcm^{-2} showed high electrical resistivity of 4.3×10^5 Ω cm and as the sputtering power was increased to 1.08 Wcm^{-2}, the electrical resistivity of the films reduced to 46 Ω cm.

From the studies outlined above, it is realized that the sputtering conditions greatly affects the electrical characteristics of thin films and can be manipulated to obtain thin films of required sheet resistivities. In addition, these conditions must be carefully monitored in order to deposit films of reproducible electrical properties as in this study. The effect of sputtering pressure was investigated using the fabricated system and the obtained measurements compared to the available experimental values. The effect of temperature variations on the film sheet resistivity was also investigated and the results compared with theoretical and other available experimental values.

CHAPTER 3

THEORETICAL CONSIDERATIONS

3.1 Introduction

Thin films are mainly deposited on substrates by physical or chemical means. This chapter outlines the theory on deposition techniques and more specifically on sputtering as it is the technique adopted in this study. Also presented are theoretical backgrounds on thin film resistivity measurement, computer interfaces and interfacing done in LabVIEW programming environment.

3.2 Deposition Techniques

Deposition techniques for thin films broadly fall in five categories: Physical vapour deposition (PVD), Chemical vapour deposition (CVD), Oxidation, Spin coating and Plating. In PVD technique, films are formed by atoms that are directly transported from source to the substrate through gas phase and they include sputtering, evaporation (Thermal evaporation and E-Beam evaporation) and Reactive PVD. On the other hand, in CVD technique, films are formed by chemical reaction on the surface of the substrate and they include Low-Pressure CVD (LPCVD), Plasma-Enhanced CVD (PECVP), Atmosphere-Pressure CVD (APCVD) and Metal-Organic CVD (MOCVD). Evaporation and sputtering are the two main techniques employed in physical vapour deposition. In this study, due to its advantages such as proper control on the film chemical composition, high deposition rate and low substrate heating during film deposition, DC reactive magnetron sputtering technique has been adopted and is discussed in the next section.

3.2.1 Sputtering Technique

Sputtering is a physical vapor deposition (PVD) technique whereby bombarding particles incident on a target collide with surface atoms thus dislodging them from the lattice through a transfer of energy (Ohring, 1992). The displaced lattice atoms as well as the bombarding particles (projectile) then undergo collisions with other lattice atoms, dislodging them and a chain reaction of collision ensues. Atoms with sufficient energy required to overcome the surface potential called the surface binding energy (U_o) will escape (Matsunanmi *et al*., 1980). The schematic diagram below shows sputtering phenomenon.

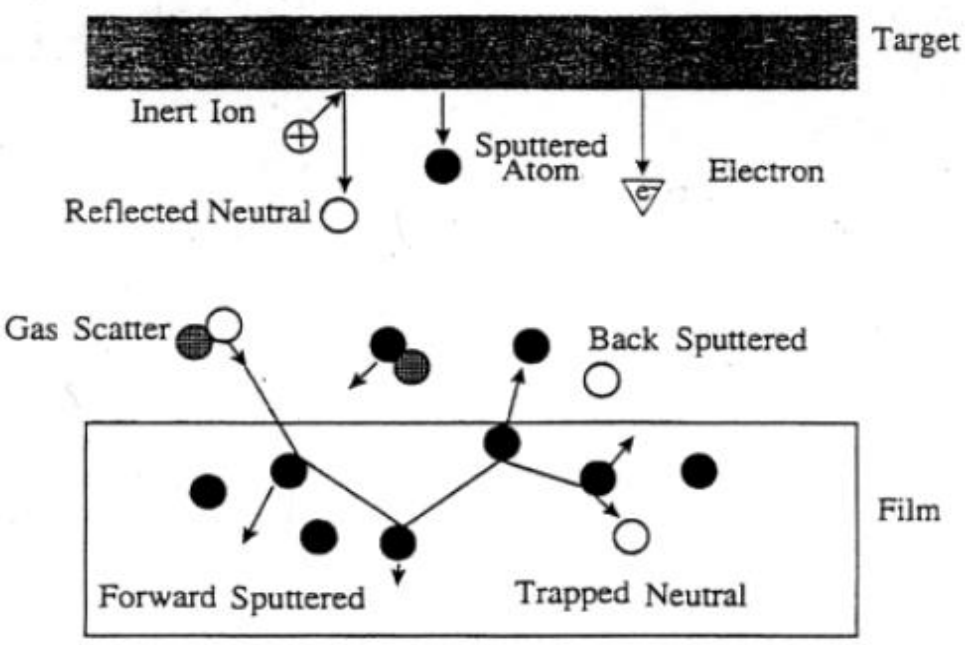

Fig. 3.1: Outline of sputtering phenomenon (Matsunanmi *et al*., 1980).

There is a minimum projectile kinetic energy needed to induce sputtering called threshold energy (E_{th}) and is given by Bohdansky (1984) as:

$$E_{th} = \frac{U_o}{\beta(1-\beta)} \quad for \quad \frac{M_1}{M_2} \leq 0.3 \tag{3.1}$$

where M_1 is projectile mass, M_2 is mean molecular mass per atom of a target and β is maximum fractional energy transfer possible in a head-on collision given by:

$$\beta = \frac{4M_1M_2}{(M_1+M_2)^2} \tag{3.2}$$

$$\text{and for } \frac{M_1}{M_2} > 0.3, \; E_{th} = 8U_0\left(\frac{M_1}{M_2}\right)^{1/3} \tag{3.3}$$

Sputtering processes are wide and varied. They can be divided up into four categories; DC, RF, magnetron and reactive. There are also important variants within each category for example DC bias and even hybrids between categories. (Almen and Bruce, 1961).

3.2.2 Other Deposition Techniques

3.2.2.1 Vacuum Evaporation Technique

Vacuum evaporation is also a widely used PVD technique. It is where materials from a thermal vaporization source reaches the substrate with little or no collision with gas molecules in the space between the source and substrate. The vacuum environment during evaporation provides the ability to reduce gaseous contamination in the deposition system to a low level. This technique is generally done using thermally heated sources

such as tungsten wire coils or by high energy electron beam heating of the source material itself. Generally, the substrates are mounted at an appreciable distance away from the evaporation source to reduce radiant heating of the substrate by the vaporization source. Figure 3.2 depicts a schematic of evaporation phenomenon.

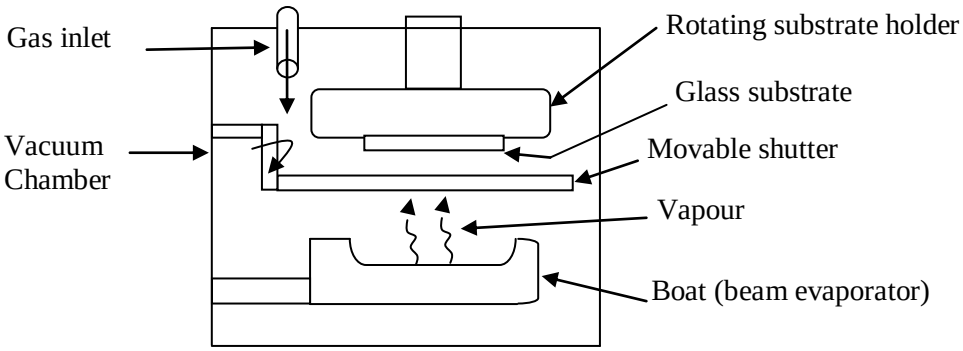

Fig. 3.2: A schematic of vacuum evaporation phenomenon

3.2.2.2 Arc Vapour Deposition Technique

Arc vapour deposition uses a high current, low-voltage arc to vaporize a cathodic electrode (cathodic arc) or anodic electrode (anodic arc) and deposit the vaporized material on a substrate. The vapourized material is highly ionized and usually the substrate is biased so as to accelerate the ions to the substrate surface.

3.2.2.3 Ion Plating Technique

Ion plating utilizes concurrent or periodic bombardment of the depositing film by atomic-sized energetic particles, to modify and control the properties of the depositing film. In

ion plating the energy, flux and mass of the bombarding species along with the ratio of bombarding particles to depositing particles are important processing variables.

3.2.2.4 Chemical Vapour Deposition Technique

Thermal chemical vapour deposition is the deposition of atoms or molecules by the high temperature reduction or decomposition of a chemical vapour precursor species which contains the material to be deposited. Reduction is normally accomplished by hydrogen at an elevated temperature. Decomposition is accomplished by thermal activation. The deposited material may react with other gaseous species in the system to give compounds (e.g. oxides, nitrides). CVD technique has numerous other names and adjectives associated with it such as Vapour Phase Epitaxy (VPE) when CVD is used to deposit single crystal films, Metalorganic CVD (MOCVD) when the precursor gas is a metal-organic species, Plasma Enhanced CVD (PECVD) when a plasma is used to induce or enhance decomposition and reaction, and Low Pressure CVD (LPCVD) when the pressure is less than ambient.

3.3 Thin Film Resistivity Measurement

3.3.1 Four Point Probe set up

Four point probe set up usually consists of four equally spaced tungsten metal tips with finite radius. Each tip is supported by springs on the other end to minimize sample damage during probing. The four metal tips are part of an auto-mechanical stage which travels up and down during measurements (Masato *et al.*, 1993). A high impedance

current source is used to supply current through the outer two probes and a voltmeter used to measure the voltage across the inner two probes as shown in figure 3.3. These values of sourced current and measured voltage are used to determine the sample resistivity. Typical probe spacing *S* is about 1 mm.

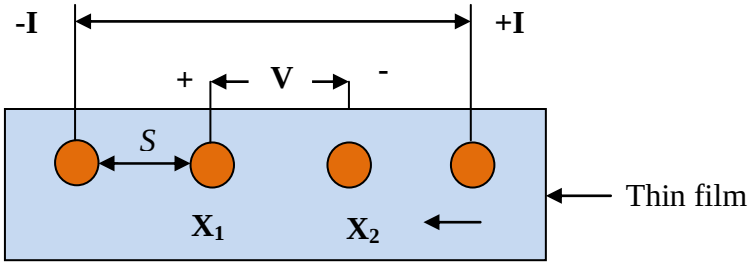

Fig. 3.3: A schematic of 4-point probe configuration with linear symmetry

3.3.1.1 Bulk sample

For bulk samples, it is assumed that the metal tip is infinitesimal and samples are semi-infinite in lateral dimension. When the sample thickness $t >> S$, the probe spacing, a spherical protrusion of current emanating from the outer probe tips is assumed. The differential resistance is given by:

$$\Delta R = \rho_s \left(\frac{dx}{A}\right) \tag{3.4}$$

where ρ_s is the sheet resistivity, A is area of the film and dx is the distance between x_1 and x_2. When integration is carried out between the inner probes where the voltage is measured, we obtain:

$$R_s = \int_{x_1}^{x_2} \rho \frac{dx}{2\pi x^2} \tag{3.5}$$

$$R_s = \frac{\rho}{2\pi}\left(-\frac{1}{x}\right)\Big|_{x_1}^{x_2} \tag{3.6}$$

$$R_s = \frac{\rho}{2\pi}\left(-\frac{1}{x}\right)\Big|_{S}^{2S} \tag{3.7}$$

$$R_s = \frac{\rho}{2\pi}\frac{1}{2S} \tag{3.8}$$

where *S* is probe spacing and is kept uniform. Due to the superposition of current at the outer two tips, *R = V/2I*. Thus, we arrive at the expression for bulk resistivity as:

$$\rho_s = 2\pi S\left(\frac{V}{I}\right) \tag{3.9}$$

3.3.1.2 Thin Film Sample

Considering a thin film with a square geometry as in figure 3.4, for a very thin layer (thickness, *t*<< probe spacing, *S*), current rings instead of spheres are got (Brown and Jakeman, 1996).

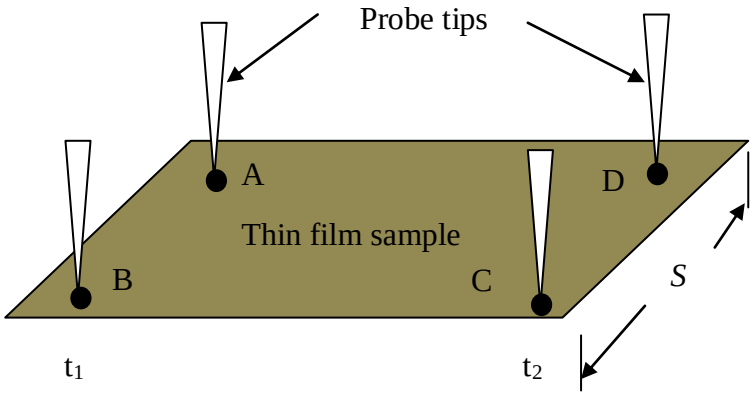

Fig. 3.4: Probe tips on film sample surface with square geometry

Therefore, the area,

$$A = 2\pi xt \quad \text{where } t \text{ is the film thickness} \tag{3.10}$$

$$R_s = \int_{x_1}^{x_2} \rho \frac{dx}{2\pi xt} \tag{3.11}$$

$$= \int_{S}^{2S} \frac{\rho}{2\pi t} \frac{dx}{x} \quad \text{where } S \text{ is the probe spacing} \tag{3.12}$$

$$= \frac{\rho}{2\pi t} \ln(x)\Big|_{S}^{2S} \tag{3.13}$$

$$= \frac{\rho}{2\pi t} \ln 2 \tag{3.14}$$

Consequently, for R= $\frac{V}{2I}$, the sheet resistivity of the thin film sheet is given by:

$$\rho_s = \frac{\pi t}{\ln 2}\left(\frac{V}{I}\right) \tag{3.15}$$

It is noted that this expression is independent of the probe spacing *S*. Furthermore, this latter expression is frequently used for characterization semiconductor layers, such as a diffused N+ region in a p-type substrate. In general, sheet resistivity can be expressed as:

$$\rho_s = K\left(\frac{V}{I}\right) \tag{3.16}$$

where the factor *K* is a geometric factor. In the case of a semi- infinite thin sheet, *K* = 4.53, which is just π/ln2 from the derivation. The factor *K* will be different for non- ideal samples. So the sheet resistance and sheet resistivity can be simply expressed as in equations 3.17 and 3.18, respectively.

$$R_s = 4.532\left(\frac{V}{I}\right) \tag{3.17}$$

$$\rho_s = 4.532t\left(\frac{V}{I}\right) \tag{3.18}$$

3.3.2 Van der Pauw Method

The Van der Pauw method for measuring resistivity is used in flat, arbitrary shaped samples. The contacts should be small and placed on the circumference of the sample. The sample should also be constant in thickness and should not contain any isolated holes. A total of eight voltage measurements may be required as shown in figure 3.5. Two values of resistivity, ρ_A and ρ_B are then computed as follows:

$$\rho_A = \frac{\pi}{\ln 2}\frac{f_A t}{I}\frac{\left(V_2 + V_4 - V_1 - V_3\right)}{4} \tag{3.19}$$

$$\rho_B = \frac{\pi}{\ln 2}\frac{f_B t}{I}\frac{\left(V_6 + V_8 - V_5 - V_7\right)}{4} \tag{3.20}$$

When the above equations are simplified, equations 3.21 and 3.22 are obtained.

$$\rho_A = \frac{1.1331 f_A t}{I}\left(V_2 + V_4 - V_1 - V_3\right) \tag{3.21}$$

$$\rho_B = \frac{1.1331 f_B t}{I}\left(V_6 + V_8 - V_5 - V_7\right) \tag{3.22}$$

where ρ_A and ρ_B are resistivities in ohm cm, t is the sample thickness in cm, V_1 to V_8 represents the voltages measured by the voltmeter, I is the current through the sample in

amperes, f_A and f_B are geometrical factors based on sample's symmetry, and are related to the two resistance ratio Q_A and Q_B, given by equations 3.23 and 3.24 respectively.

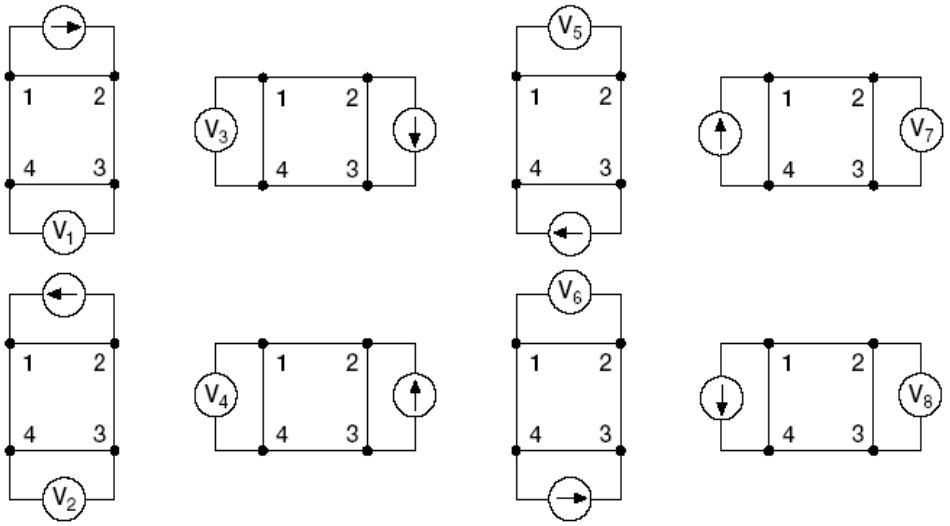

Fig. 3.5: Van der Pauw resistivity measurement conventions (Keithley Instruments Inc., 2004).

For perfectly symmetrical sample, f_A=f_B=1. Q_A and Q_B can be calculated using the measured voltages as depicted in figure 3.5.

$$Q_A = \frac{V_2 - V_1}{V_4 - V_3} \tag{3.23}$$

$$Q_B = \frac{V_6 - V_5}{V_8 - V_7} \tag{3.24}$$

Q and f are related as follows:

$$\frac{Q-1}{Q+1} = \frac{f}{0.693} ar\cosh\left(\frac{e^{0.693/f}}{2}\right) \tag{3.25}$$

A plot of a symmetry factor, *f* as a function of correction factor, *Q* is depicted in figure 3.6.

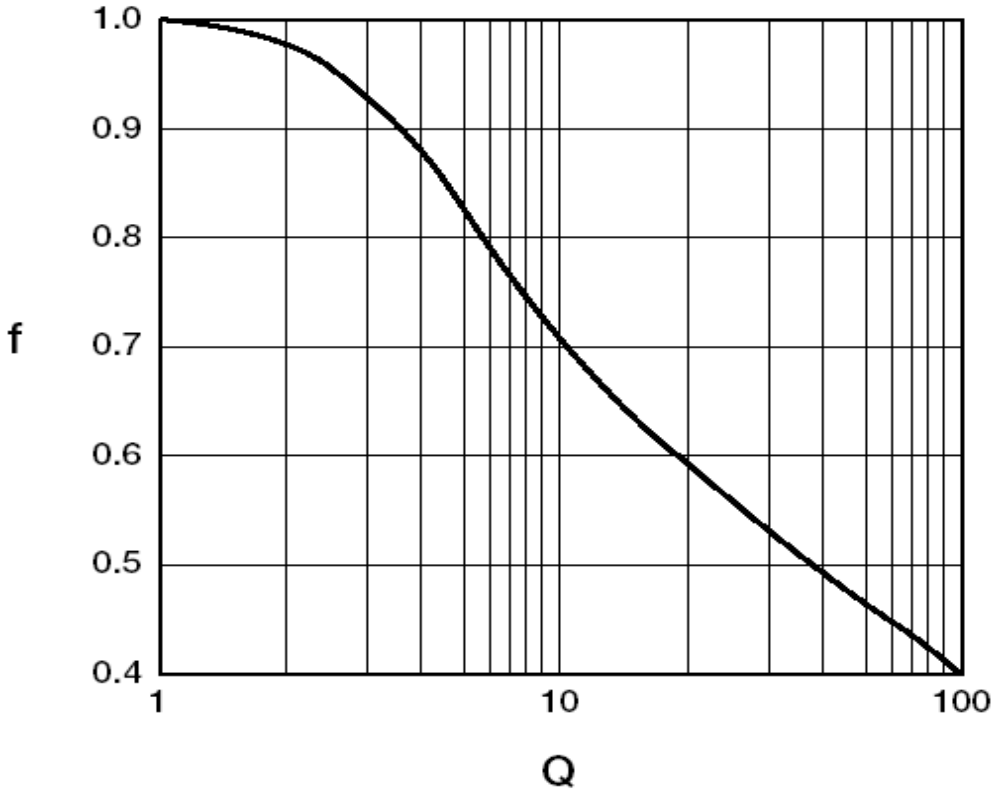

Fig. 3.6: A plot of f as a function of Q (Keithley Instruments Inc., 2004)

It is noted that if ρ_A and ρ_B are not within 10% of one another, the sample is not sufficiently uniform to accurately determine its resistivity. Once ρ_A and ρ_B are known, the average resistivity ρ_{av} can be determined as follows:

$$\rho_{av} = \frac{\rho_A + \rho_B}{2} \tag{3.26}$$

In this way, the resistivity of arbitrary shaped samples can be measured. When only two probes are performed, the sheet resistance is given by equation 3.27.

$$R_s = \frac{\pi}{\ln(2)} f(Q) \frac{V_{BC} + V_{DC}}{2I} \left[\Omega / Square \right] \quad (3.27)$$

where *f* and *Q* are the Van der Pauw symmetry and correction factors respectively. *Q* is given by conditions in equation 3.28.

$Q = V_{DC}/V_{BC}$ for $V_{BC} \leq V_{DC}$, while $Q = V_{BC}/V_{DC}$ for

$$V_{BC} \geq V_{DC} \quad (3.28)$$

f is a function of *Q* which is valid for $Q < 10$ and it is expressed in the form:

$$f = 1 - 0.34657\left(\frac{Q-1}{Q+1}\right)^2 - 0.09236\left(\frac{Q-1}{Q+1}\right)^4 + ... \quad (3.29)$$

Equation 3.29 is obtained by performing cosh expansion of equation 3.25 in order to express the symmetry factor, *f* in terms of the correction factor, *Q*. Taking only the first two terms of equation 3.29 since the proceeding terms are negligible, equation 3.30 is achieved.

$$f = 1 - \frac{\ln 2}{2}\left(\frac{Q-1}{Q+1}\right)^2 \quad (3.30)$$

The sheet resistivity (ρ_s) can be expressed in terms of the film thickness, *t* in nanometres and the sheet resistance, R_s as depicted in equation 3.31.

$$\rho_s = R_s \, 10^2 \, t \ \Omega \text{ cm} \quad (3.31)$$

3.4 Computer Interfaces

Interfacing is the process of making two or more devices or systems operationally compatible with each other so that they function together as required (Gregor, 2007).

There are many ways to interface a device to a computer with standard built-in ports offering a practical and easier alternative. This section presents available computer ports and LabVIEW software used as interfacing environment in this study.

3.4.1 Computer Ports

Ports are external connections to a computer. There is need for interaction between a computer and a peripheral device. This is called interfacing. Automation is an interfacing technique which provides interaction between a computer or any intelligent device and laboratory equipment, to get reliability, accuracy and remote operation. Computers are digital machines as they can only accept ‘zeros’ or ‘ones’. Zero (0) represents zero state in binary system (i.e. 0-2.5 volts state) and one (1) represents one state (i.e. 2.5-5.0 volts state). This voltage standard level is called TTL logic levels.

Since the physical variables are in analogue form, the first step of interfacing requirement is analogue to digital (binary) conversion of the physical quantity to be monitored. Once the variables become digital information, it is easy to interact with a computer for further connectivity of the system which contains various physical quantities or variables to be monitored and measured. Various interfacing techniques can interact with the computer for experimental automation. Some of them are serial interface, parallel interface, Universal Serial Bus (USB) interface, Ethernet, GPIB and game port interface among others.

3.4.1.1 Serial Port (RS-232)

Serial ports being one of the oldest of the interface standards complies with the RS-232 standard. They are nine-pin connectors that relay information, incoming or outgoing, one bit at a time. Each byte is broken up into a series of eight bits, hence the term serial port. Before internal modems became commonplace, external modems were connected to computers via serial ports, also known as communication or 'COM' ports. Computer mice and keyboards also use serial ports. Some serial ports use 25-pin connectors, but the nine-pin variety is more common. Serial ports are controlled by a special chip called a UART (Universal Asynchronous Receiver Transmitter). Figure 3.7 shows a 9-pin computer port pinout.

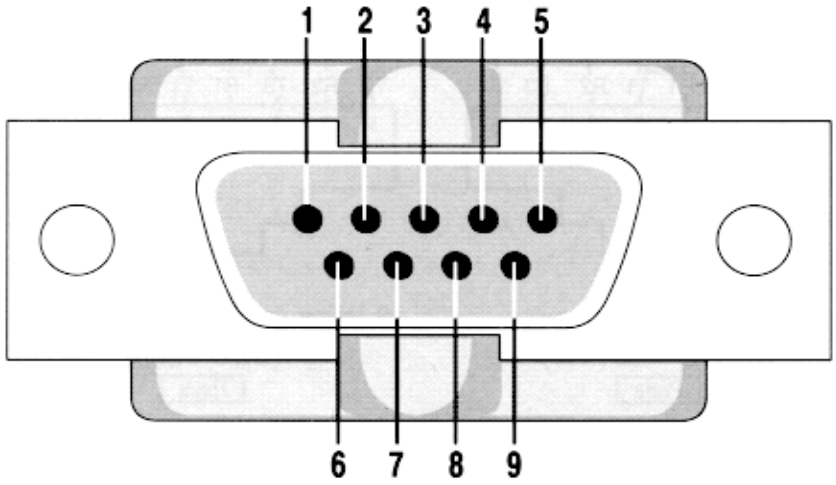

Fig. 3.7: 9-pin computer serial port pinout diagram (Gregor, 2007)

Table 3.1 provides pinout identification for the 9-pin (DB-9) as shown in figure 3.7. Also shown in the table is 25-pin (DB-25) serial port connector pinout.

Table 3.1: Serial port pinout identification for DB-9 and DB-25 connectors

DB-9 Pin number	DB-25 Pin number	Signal
1	8	DCD, data carrier detect
2	3	RXD, receive data
3	2	TXD, transmit data
4	20	DTR, data terminal ready
5	7	GND, signal
6	6	DSR, data set ready
7	4	RTS, request to send
8	5	CTS, clear to send
9	22	R1, ring indicator

3.4.1.2 Parallel port (LPT)

The LPT (Line Printing Terminal) is a common name given to a parallel port on most computers. Although the DB-25 female connector at the back of a computer is referred to as an LPT port, technically an LPT port is simply a parallel port set to LPT(x) with an input/output address and an Interrupt Request (IRQ) assigned to it, in the same way as a COM(x) port is actually a serial port set to COM(x). Many computers have two LPT ports, although some have up to three LPT ports; LPT1, LPT2 and LPT3. These ports were designed primarily for printers but today, a wide variety of peripherals can be

connected to these ports. A standard parallel port transmits eight data bits at a time, as opposed to a serial port which transmits data one bit at a time. Due to its speed advantage over the serial port, parallel ports are commonly used for printers and even small networks. ECP (Extended Capability Port), EPP (Enhanced Parallel Port) and Standard Parallel Port (SPP) or bi-directional are the common implementations of the parallel port standard. They offer faster data transfer of up to 2 Mb/s and are commonly supported in modern computers.

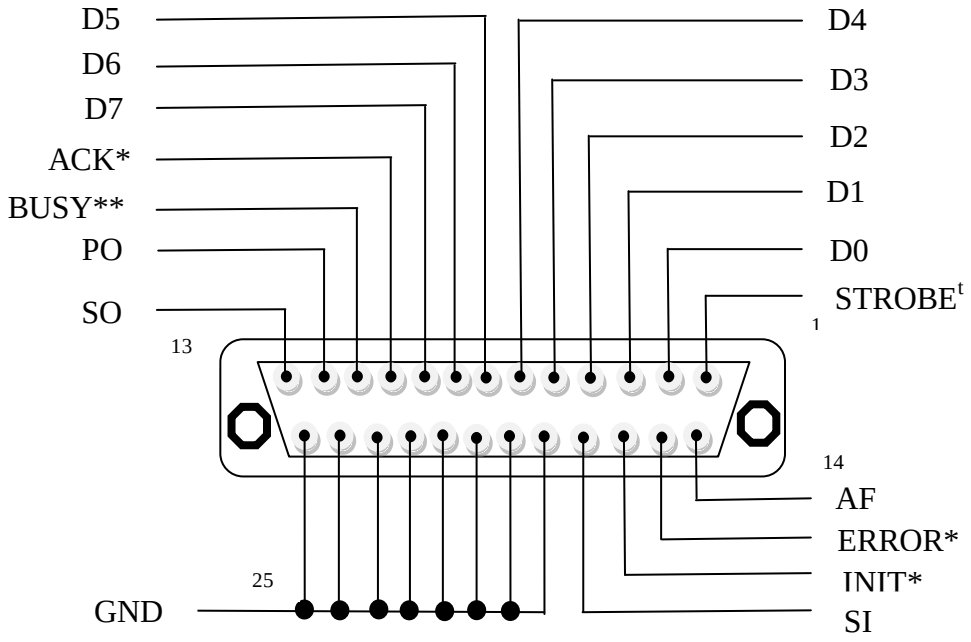

Fig. 3.8: Computer printer port pinout (Markham, 1993)

There are three types of pins as summarized in the table 3.2 showing parallel port pinouts: data pins (input in bidirectional mode/output, I/O), status pins (input only, I) and control pins (output only, O). Status pins are used to allow the printer or other external circuit to signal the computer. Control pins are used to allow the computer to control the printer or an external circuit. Finally, data pins are Transistor-Transistor-Logic (TTL)

outputs and generate a typical logic HIGH of 2.5V-5V DC and a logic LOW of 0-2.5V. These pins can be used to send or receive data, or may be used in the same manner as the status and control pins.

Table 3.2: Label and description of printer port pinout as shown in figure 3.8

Pin	Name	Description	Address/Bit	I/O
1	STROBE[t]	Strobe. Inform printer that data on D0-D7 are valid	Base+2, Bit 0	I/O
2	D0	Data bit 0. Data bus	Base+0, Bit 0	I/O
3	D1	Data Bit 1. Data bus	Base+0, Bit 1	I/O
4	D2	Data Bit 2. Data bus	Base+0, Bit 2	I/O
5	D3	Data Bit 3. Data bus	Base+0, Bit 3	I/O
6	D4	Data Bit 4. Data bus	Base+0, Bit 4	I/O
7	D5	Data Bit 5. Data bus	Base+0, Bit 5	I/O
8	D6	Data Bit 6. Data bus	Base+0, Bit 6	I/O
9	D7	Data Bit 7. Data bus	Base+0, Bit 7	I/O
10	ACK	Acknowledge. Notify the Computer that the printer is ready to receive the	Base+1, Bit 6	I

		next set of data		
11	BUSY**	Printer buffer full or printer busy. The computer needs to wait until this line is set high before transmitting again	Base+1, Bit 7	I
12	PO	Paper Out. Printer is out of paper	Base+1, Bit 5	I
13	SO	Select out. Printer is on line and is ready	Base+1, Bit 4	I
14	AF	Auto Feed. Printer line feed	Base+2, Bit 1	O
15	ERROR*	Error. The printer has an error	Base+1, Bit 3	I
16	INIT*	Reset. Initialize the printer	Base+2, Bit 2	O
17	SI	Select In. Send a signal to the printer	Base+2, Bit 3	O
18-25	GND	Ground	--	--

3.4.1.3 Universal Serial Bus (USB)

Today, there is a growing use of USB interface. Just about every peripheral made now comes with a USB version. A sample list of USB devices that are in the market today includes printers, scanners, mice, joysticks, flight yokes, digital cameras, webcams, scientific data acquisition devices, modems, speakers, telephones, video phones, storage devices such as zip drives and network connections. The USB interface is an ultrafast design, meant for any specific requirement with the common interfacing standard to enable interconnectivity of any USB enabled system to the computer. It provides a single, standardized, easy-to-use way to connect up to 127 devices to a computer.

3.4.1.4 GPIB (IEEE 488)

Traditionally, the communication interface of choice for instrument control has been the IEEE 488, General-Purpose Interface Bus (GPIB). It is a digital, 8-bit parallel communication interface with data transfer rate of up to 8 Megabytes per second. The bus provides one system controller for up to 14 instruments and cabling is limited to less than 20 m. Users can overcome both of these limitations by using GPIB expanders and extenders. GPIB cables and connectors can be industrially shielded for use in noisy environments. Other ports commonly used in computers include Ethernet and IEEE 1394 (Firewire) ports.

CHAPTER 4

MATERIALS AND METHODS

4.1 Introduction

A four point probe head used for sheet resistivity measurement being commercially expensive and not easily available has been designed and fabricated. A relay switching device to perform switching of probe tips on the thin film sample surface as per Van der Pauw set-up has also been designed and fabricated. This chapter outlines the materials used for these designs and the fabrication methodologies. Due to need for computer-aided control of the fabricated switching device and the Keithley SourceMeter unit, how they are interfaced using LabVIEW software via the computer parallel port (LPT1) and serial port (RS-232 port) respectively are also presented. The deposition of the Cu_2O thin films on glass substrates under different conditions by DC reactive magnetron sputtering technique and the sheet resistivity measurement of the deposited thin films using the fabricated system are also outlined in this chapter.

4.2 Four Point Probe Head Design and Fabrication

The fabrication of this system was done using Perspex sheets, steel bolts, aluminum rods, spiral springs, metallic tubes, fastening screws, connecting cables and crocodile clips. Four holes 0.5 cm apart were drilled on a Perspex sheet measuring 12 cm by 12 cm and steel bolts inserted in the four holes ensuring that the spacing between them is equal and maintained. Four spring loaded metallic tubes were connected to the four aluminum rods with sharp ends to act as probing tips on one side and to the steel screws on the other end.

The perspex sheet mounted with the probe tips was able to move up and down about another perspex sheet stage for holding the thin film whose sheet resistivity is to be measured when tapping screws were loosened. Figure 4.1 shows a schematic of the fabricated probe head.

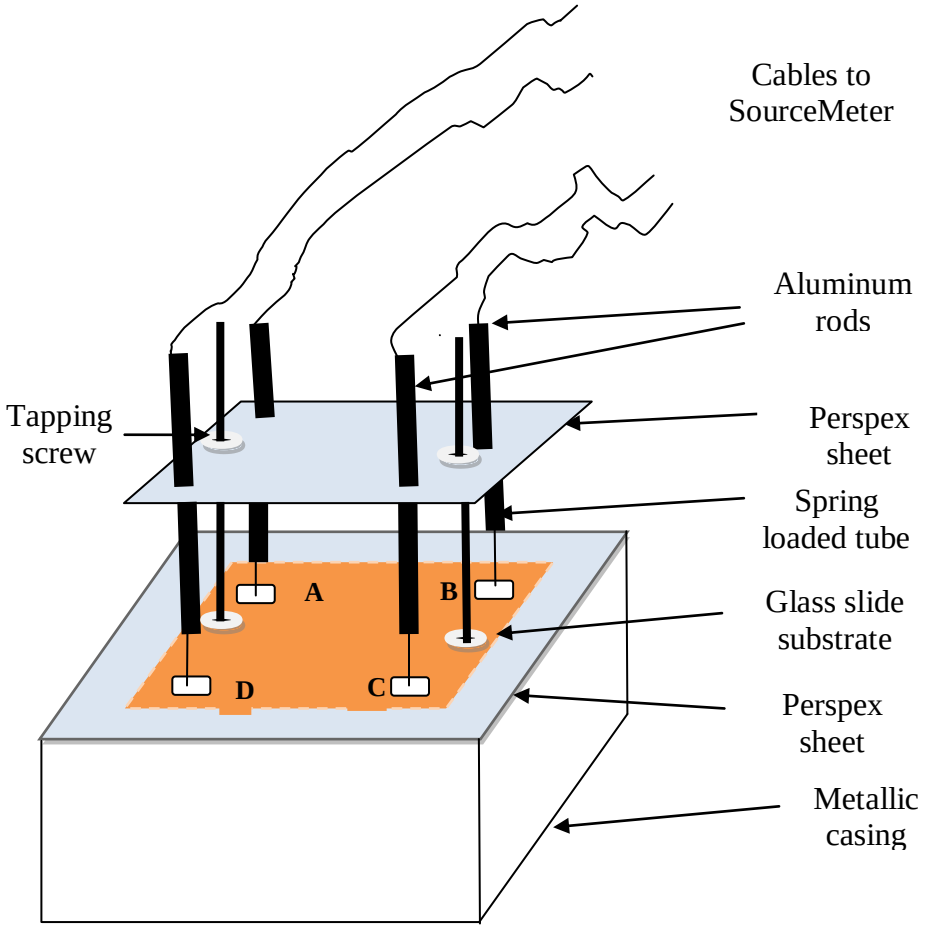

Fig. 4.1: Schematic of fabricated probe head for use in sheet resistivity measurements

4.3 Van der Pauw Switching Device Design

An electronic switching device was designed and fabricated to perform switching of probe tips on the sample as outlined by the Van der Pauw set-up. This was accomplished

by use of a transistor driven 14-pin relay switch controlled by a computer via printer port (LPT1). Transistor Q_2 in positive ground mode was used as a switching transistor with its collector connected to the base of another transistor Q_1 which is the load transistor. Transistor Q_1 was used to amplify the load current. The base resistor R_2 was used to control the switching current that goes to the relay coil. Its value was calculated from the knowledge of load current I_C and the transistor transfer characteristics H_{FE} available in the datasheets. Resistor R_3 was used to stabilize the base of Q_2 and to ensure that the transistor completely switches off. It ensures that the transistor base does not go slightly negative which may cause a very small amount of collector current to flow. Diode D_1 in reverse bias was connected in parallel with the relay coil. This was to prevent the kickback voltage that occurs momentarily when the normal current stops flowing through the coil from destroying the switching transistor.

The PNP transistor was used as the load transistor. The base of the switching transistor was connected to the computer's printer port data pin via PC817 optoisolator to isolate the two circuits and hence protect the computer from any damage. When the transistor base voltage was sent HIGH from the computer's port voltage of approximately +3.3V by setting it to logical 1, transistor Q_2 was fully switched ON hence current was allowed to flow to the base of the load transistor. This in turn switched on the load transistor Q_1 allowing current flow on the relay coil switching it ON. When the computer port was at logical zero, the converse happened since zero volts was applied to the base of Q_2. The load resistor was in turn switched off keeping the relay OFF. Figure 4.2 shows the Van der Pauw switching device designed in ExpressSCH software.

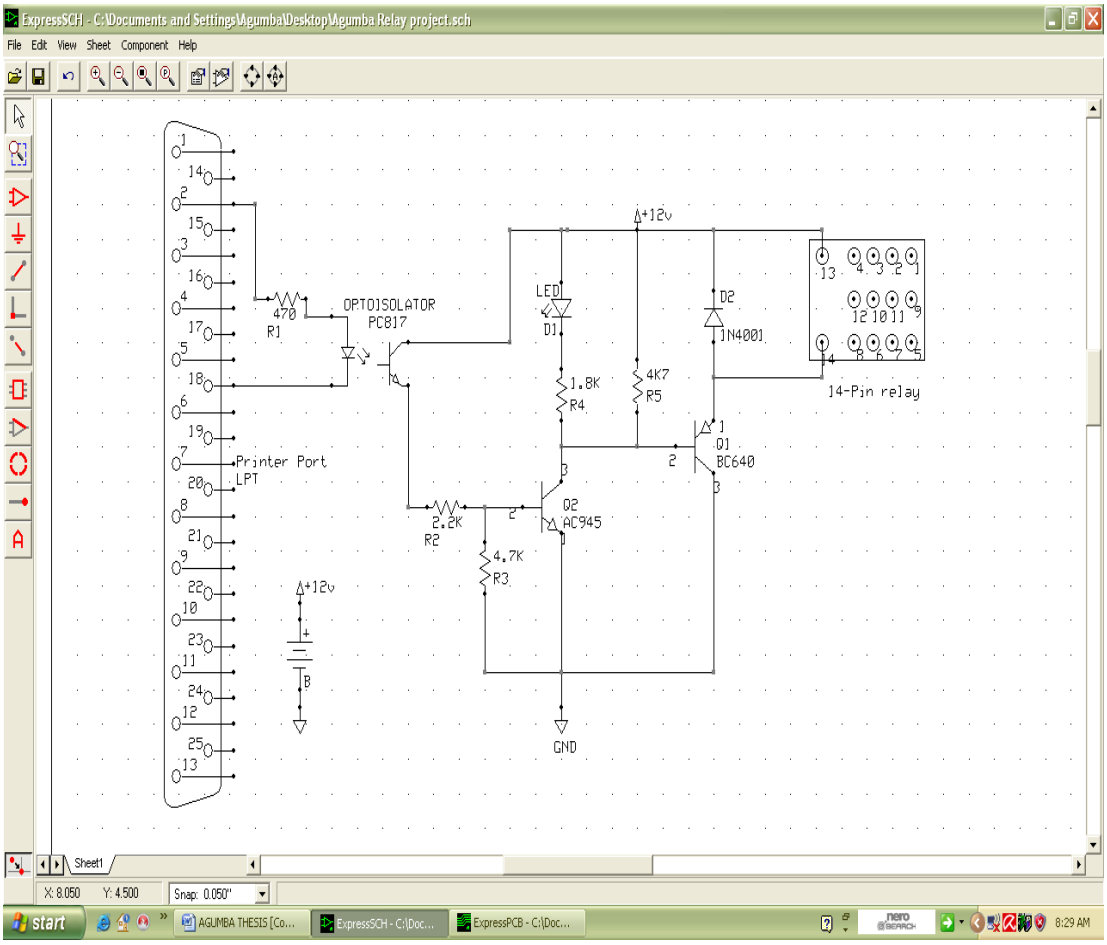

Fig. 4.2: Design diagram of relay switching device circuit

4.4 Device Interfacing Techniques Using LabVIEW

There was need for interaction between the computer, the Keithley SourceMeter unit and the relay switching device. The interfacing was done to provide automation of measurements by enhancing data flow between the computer and the peripherals (SourceMeter and the switching device). There was hence a full control of the peripheral devices by the computer. This was done in an interactive LabVIEW environment using VISA VIs (Virtual Instruments Software Architecture). It is a standard Input/Output Application Programming Interface (API) for instrumentation programming. It can

control VXI, General Purpose Interface Bus (GPIB), or serial instruments, by making the appropriate driver calls depending on the type of instrument being used. Figure 4.3 shows National Instruments Virtual Instruments Software Architecture (NI-VISA) hierarchy.

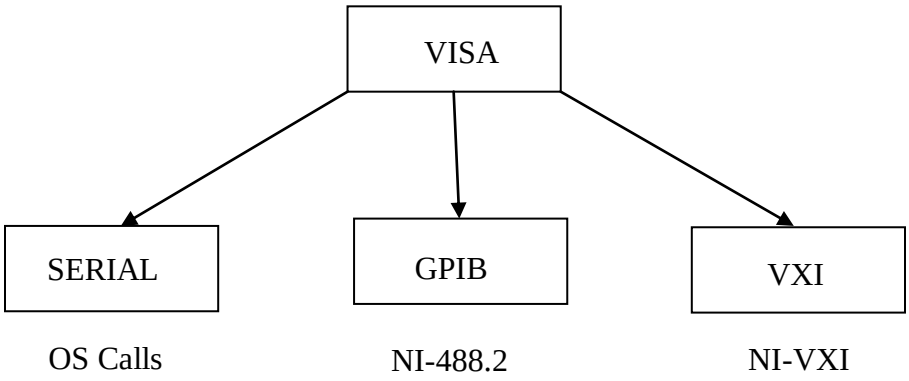

Fig. 4.3: Schematic of NI-VISA hierarchy

For Keithley SourceMeter to be controlled via the computer serial port and the switching device via parallel port respectively programming was done using LabVIEW's VISA.

4.4.1 Keithley SourceMeter Interfacing

This instrument interfacing was done via computer serial port. The instrument's RS-232 serial port was connected to the computer serial port using a straight-through RS-232 cable terminated with DB-9 connectors. First, there was need to initialize and configure the SourceMeter serial port for serial communication between it and the computer. This required the installation of 24xx VXI-PnP SourceMeter device driver installed in a computer running LabVIEW software. In this study, VISA was then used to configure the

serial port and initialize it. Due to the requirements of RS-232 serial transfer, the following configurations were done on the SourceMeter as depicted in table 4.1.

Table 4.1: Configurations to initialize SourceMeter serial port

VISA Resource name	ASRL1::INSTR
Baud rate	9600
Parity	None
Stop bits	1
Data bits	8
Terminator	<CR+LR>
Flow Control:	XON-XOFF

To allow serial port communication with LabVIEW, VISA Configure Serial Port.vi was employed. In this VI, port number used was set as COM 1 (ASRL1::INSTR) as shown in the front panel in figure 4.4.

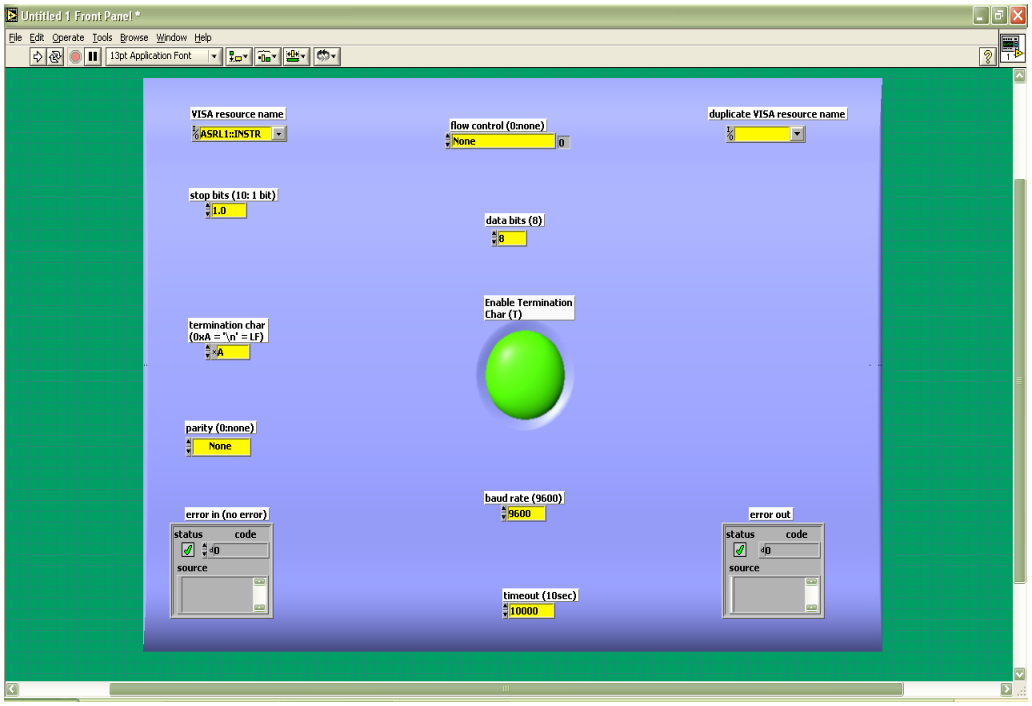

Fig. 4.4: Front panel diagram for configuring computer serial port

The other settings done are as displayed in the corresponding block diagram in figure 4.5.

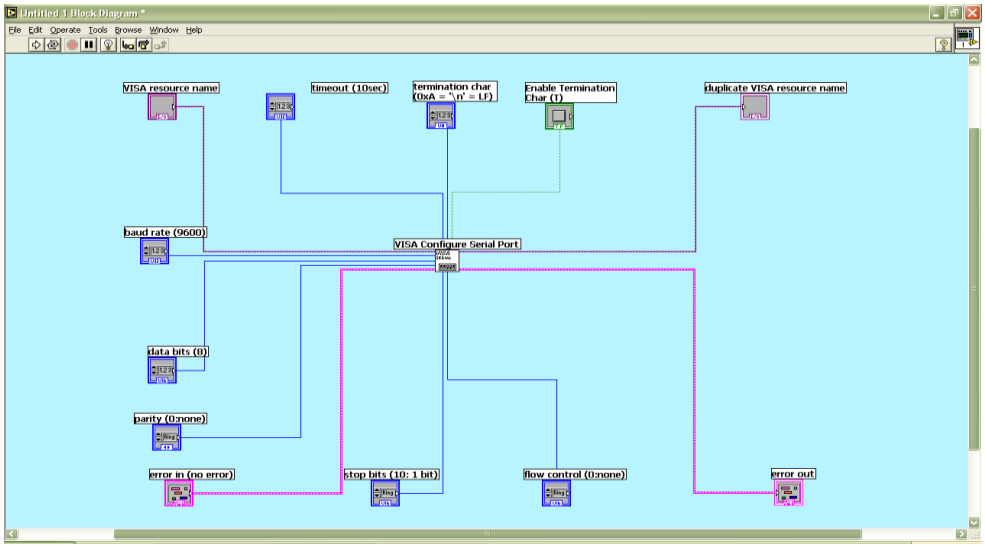

Fig. 4.5: Block diagram code for configuring the computer serial port

Once the configuration of both the computer COM1 port and Keithley SourceMeter serial port were done as in the block diagram above, a Ke24xx Initialize.vi was used to perform initialization action. The front panel in figure 4.6 indicates instrument handle, the instrument model, the instrument status and the error controls.

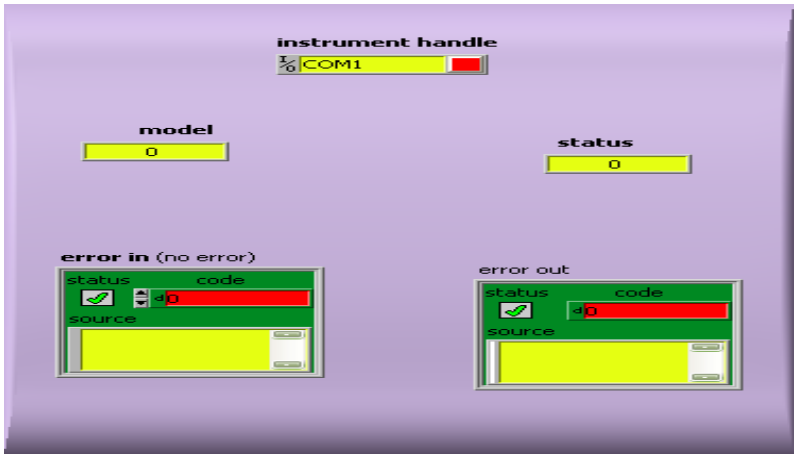

Fig. 4.6: The front panel for serial port initialization

The program code for the initialization is shown by the block diagram as depicted in figure 4.7.

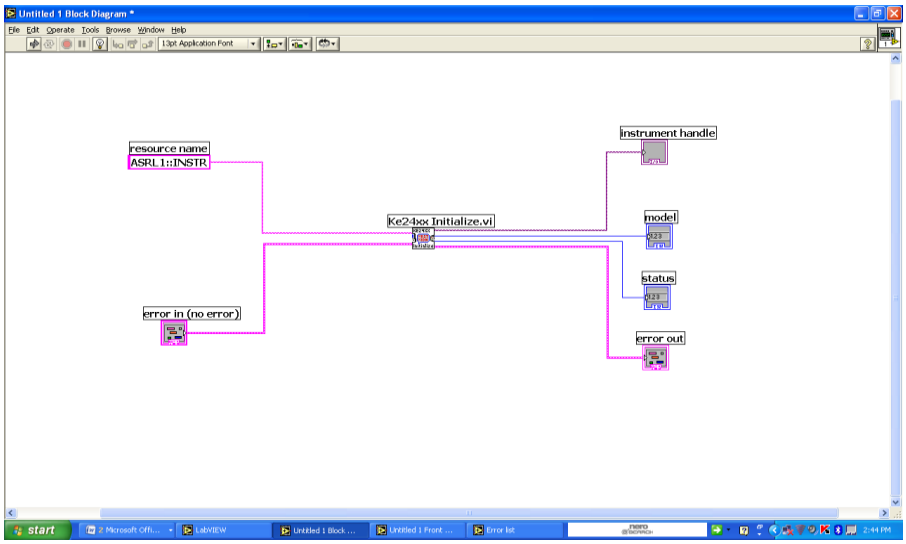

Fig. 4.7: Block diagram code to initialize the computer serial port (RS-232)

The above VI opens a session to the Default Resource Manager and a resource to the SourceMeter device using the interface ASRL1::INSTR and resets it to a known state. For different sessions of this driver, it returns a resource handle and a unique session is opened each time this function is invoked. The status control contains the status code returned by the function and the model returns the model number of the instrument (2400 model). Once these settings were done, the interface was ready for serial communication between the computer and the SourceMeter unit.

4.4.2 Van der Pauw Switching Device Interfacing

Due to the required switching of probe tips on the thin film sample surface in accordance with the Van der pauw set-up, a computer operated relay switch is used. There was hence need for communication between the computer and the device. This was achieved by interfacing the Van der Pauw switching device to the computer via the printer port (LPT1). Bi-directional (PS/2) advanced version of Standard Parallel Port (SPP) mode was set in the computer's basic input/output system (BIOS). After this setting was done, the interfaces available in the computer were checked. This was done by starting a VISA Interactive Control (VISAIC) program supplied with LabVIEW software as depicted in figure 4.8.

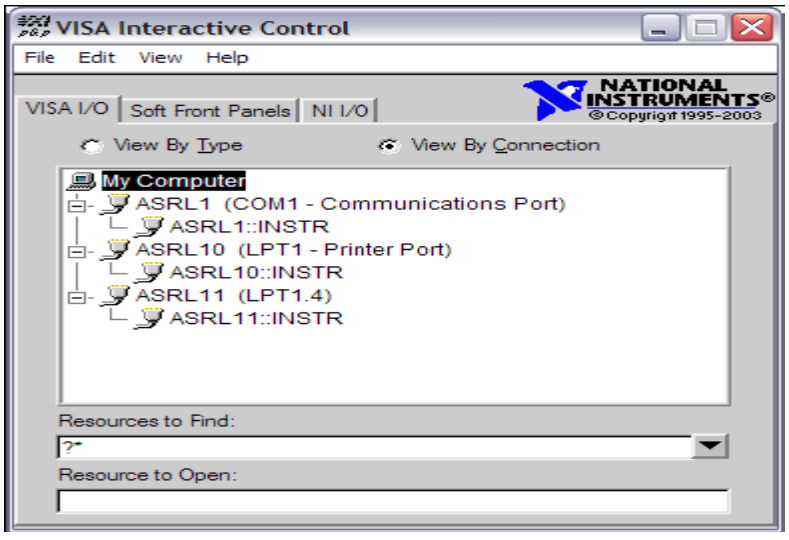

Fig. 4.8: VISA Interactive Control to check interfaces available in the computer

To access the interface control of the printer port, ASRL 10 was double clicked and the parallel port was configured to the hexadecimal base address of 0x378H. The status address was set at 0x379H and control address at 0x37AH. Data pin (pin 2) was connected to +5.0V supply of the switching circuit through an optocoupler (TDO PC 817). This component was used to safeguard the printer port from any damage caused by any wrong connection if any by separating the computer port voltage (0V-5.0V) from the external voltage (+12.0V) driving the relay switching device. The printer port ground pin (pin 18) was connected to the hardware ground terminal also via the optocoupler.

A number of LabVIEW VIs were developed to control the switching device by use of inport.vi and output.vi. These VIs were found to be compatible with window XP used as the computer's OS. The VIs were developed to turn the switching device ON and OFF. When a logical (1) was written on the outport.vi, it made data pin 2 connected to the switching device go HIGH as read from the inport.vi. A voltage of approximately +3.3V from the computer port was then sourced to the circuit setting the switching device ON as shown in the front panel in figure 4.9.

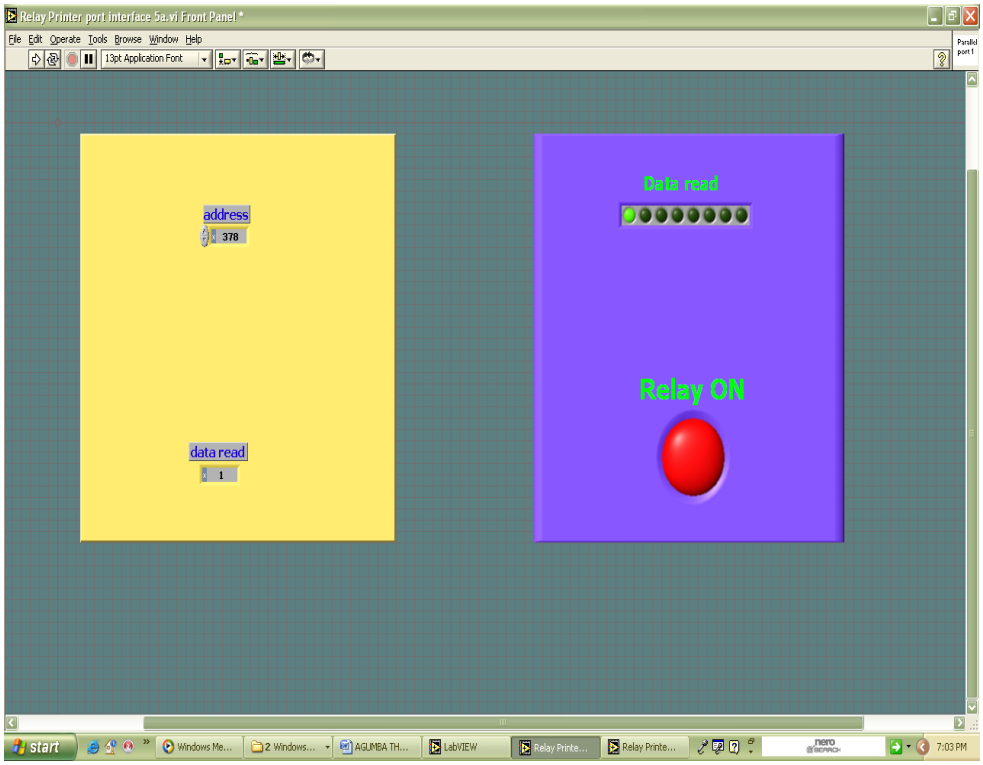

Fig. 4.9: Front panel of VI to turn the switching device ON

Figure 4.10 shows a code that was used to turn the switching device ON when it was run.

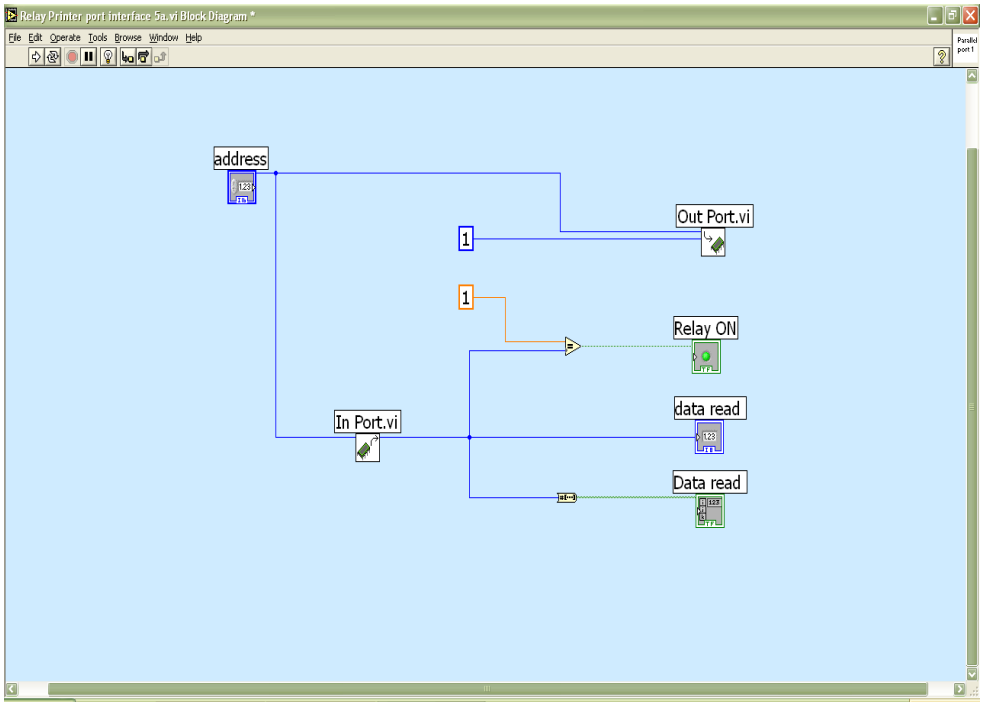

Fig. 4.10: Block diagram code to turn the switching device ON

When a logical zero (0) was written to the outport.vi, the computer data pin 2 was set LOW and read in the inport.vi. A zero volt potential was sourced to the external switching device circuit. This turned the switching device OFF as seen in the front panel in figure 4.11. The program code that was used to turn the device OFF is shown in the block diagram code in figure 4.12. Once VIs to control the Van der Pauw switching device were developed, the Cu_2O thin films whose sheet resistivity were to be measured were prepared. The next sub-section outlines how the films were deposited and how they were later used to test the workability of the fabricated system.

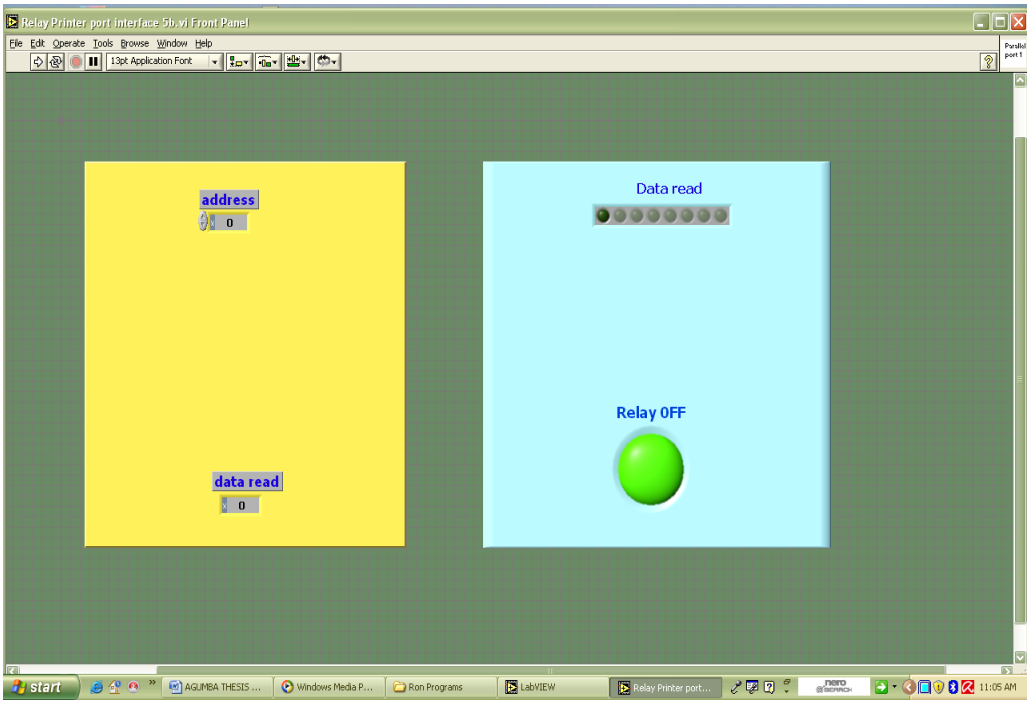

Fig.4.11: Front panel VI to turn the switching device OFF

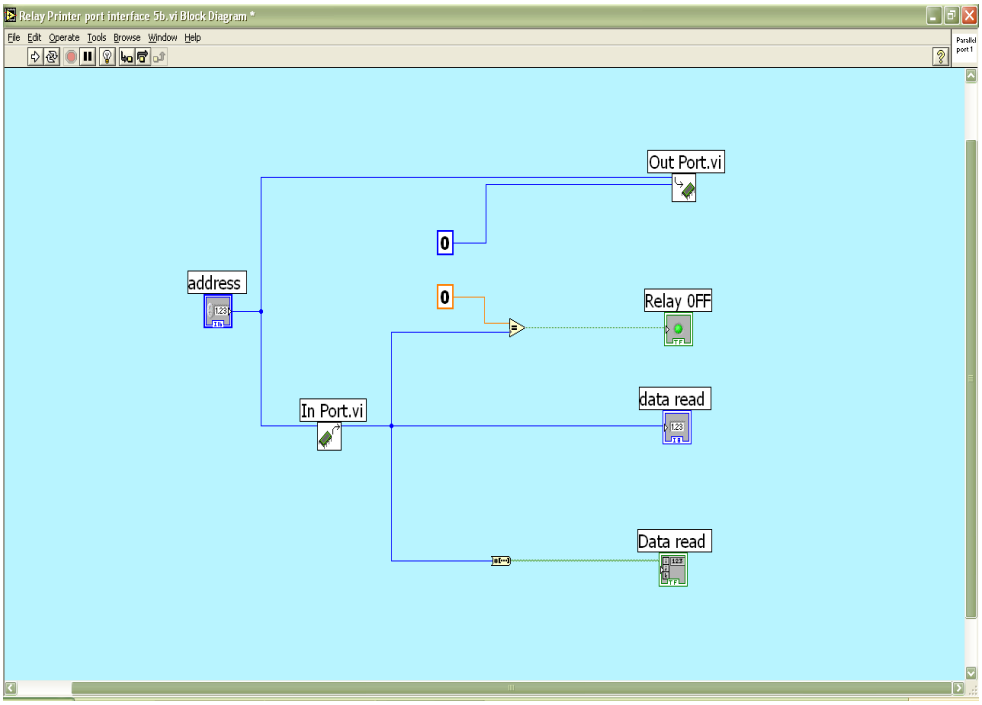

Fig. 4.12: Block diagram VI code to turn the switching device OFF

4.5 Deposition of Cu_2O Thin Films

4.5.1 Deposition of Cu_2O Test Samples

The Cu_2O films used to illustrate the workability and reliability of the designed and fabricated system were deposited on the glass substrates by DC reactive magnetron sputtering method using Edward's AUTO 306 vacuum coater. First, ultimate vacuum was created in the chamber by pumping it with diffusion pump and rotary pump combination until a base pressure of 2.5×10^{-6} mbar was measured by Pirani–Penning gauge combination. Copper target was then pres-sputtered in pure argon atmosphere for 15 minutes in order to remove oxide layers formed if any on the target with a shutter incorporated below the sputtering target to isolate the substrate during the pre-sputtering process. This is essential in the reactive sputtering to obtain the films with reproducible properties. After the pre-sputtering, oxygen gas was admitted in to the chamber until oxygen partial pressure of 2×10^{-4} mbar was achieved. Argon gas was then introduced so as to reach the required sputtering pressure of 1.9×10^{-2} mbar as it is the practiced process in reactive sputtering technique. The flow rates of both argon and oxygen gases were controlled individually by Tylan mass flow controllers operated by a LabVIEW program. A continuously variable DC power supply of 750V and 3 A was used to regulate the discharge current of 200 mA.

The substrate shutter was then removed to allow deposition of the films on the glass substrates. The argon ions (Ar^+) were accelerated towards a copper target dislodging copper atoms which reacted with oxygen atoms forming thin films of Cu_2O that was deposited on the glass substrates. The Cu_2O films were deposited at a fixed oxygen

partial pressure, substrate temperature, sputtering power and sputtering pressure as depicted in table 4.2.

Table 4.2: Sputtering conditions during Cu_2O thin film test samples deposition

Sputtering target	Pure Copper (100 mm diameter and 3mm thick) and 99.99% pure
Sputtering to substrate distance	65 mm
Base Pressure	$2.5x10^{-6}$ mbar
Oxygen partial pressure	$2x10^{-4}$ mbar
Sputtering pressure	$1.9x10^{-2}$ mbar
Substrate temperature	473 K
Cathode Current	200 mA
Sputtering Power	200 W

One hour after completing sputtering and power switched off, the deposited Cu_2O thin film samples were removed for I-V measurement and subsequent sheet resistivity measurements.

4.5.2 Deposition of Cu_2O Thin Films at Different Sputtering Pressures

In order to investigate the effect of sputtering pressure on thin film sheet resistivities using the developed system, seven samples were deposited at different sputtering pressures of 1.8 Pa, 1.9 Pa, 2.0 Pa, 2.1 Pa, 2.2 Pa, 2.3 Pa and 2.4 Pa. The other parameters

such as base pressure, oxygen partial pressure and sputtering power were maintained as outlined in table 4.2. Since thin film thickness is a vital parameter for sheet resistivity measurements, the next sub-section describes how the measurements were done.

4.6 Thin Film Thickness Measurements

For thin film sheet resistivity computation, film thickness is a very important parameter. There are many techniques for thickness measurement such as ellipsometry, interferometry, quartz crystal oscillators and stylus-method profilometry among others (Ohring, 2002). In this study, the latter technique was adopted. The method consists of measuring the mechanical movement of a diamond needle (stylus) as it is made to trace the topography of the film- substrate step. The steps were created during the films deposition by masking parts of the substrates with aluminum foil before deposition. To measure thickness, thin films were placed on the profilometer device stage and then fine stylus draged across the film surface. When the stylus encountered a step, signal variations (based on a differential capacitance or inductance technique) indicated the step height. This information was then displayed on a computer screen as film thickness.

4.7 Thin Film Sheet Resistivity Measurements

After the system was fully developed and interfaced to a computer for automatic control, it was now used to perform sheet resistivity measurement of the deposited thin films.

4.7.1 Four Point Probe Technique for Sheet Resistivity Measurement

Four point probe technique was used to measure the sheet resistivity of the Cu_2O semiconductor thin film samples. With a symmetrical square geometry adopted, the four leads from the designed probe head were connected to Keithley SourceMeter via the switching device as per the Van der Pauw set-up for Voltage and Current measurements. The schematic diagram of four-point probe resistivity measurement is depicted in figure 4.13.

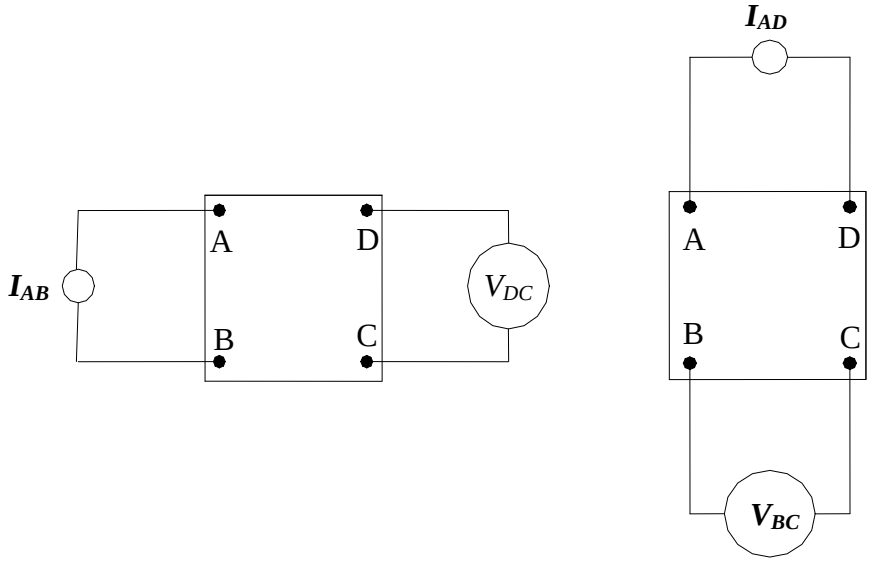

Fig. 4.13: A schematic of four-point probe resistivity measurement-Van der Pauw method

A current of 1.0 x 10^{-10} A was applied through the contacts A and B and the potential drop V_{DC} across the contacts D and C measured. With switching of probe tips on the sample done by the developed switching device, the same amount of current (I) was then applied through the contacts A and D and the potential drop V_{BC} across the contacts B

and C measured. These values of current, measured voltage drops and film thickness were used to compute sheet resistivity by the developed LabVIEW software. The sheet resistivity measurement of the test sample was first performed at room temperature (23^{o}C) and then at varied temperatures by placing the sample in a Lindberg/Blue Tube Furnace TF55035A model. Sheet resistivities of thin films deposited at different sputtering pressures were then measured using the technique by repeating the above procedures.

4.7.2 Van der Pauw Switching on the Thin Film Surface

This was achieved by use of a switching device which was basically a transistor operated 14-pin relay switch controlled by a computer via printer port (LPT 1). Figure 4.14 shows a schematic diagram of a 14-pin relay used to perform a Van der Pauw switching on the thin film sample.

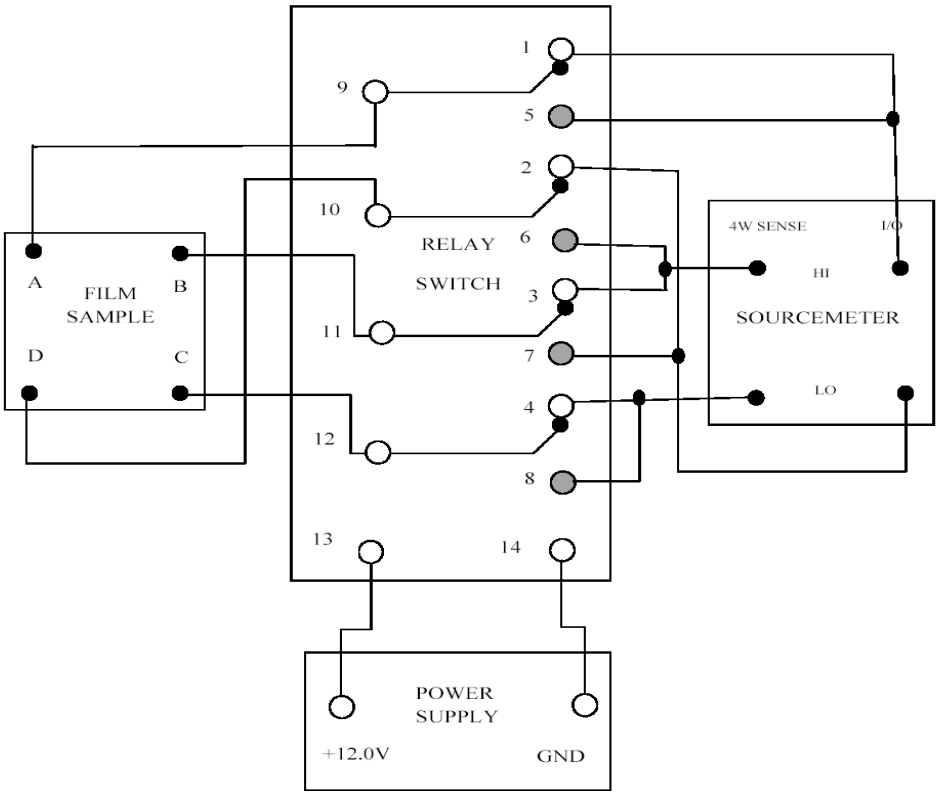

Fig. 4.14: Schematic of 14-pin relay switching as per Van der Pauw set-up

With the relay on default OFF mode, point A of the sample is connected to the SourceMeter I/O HI via pins 9 and 1. Point B is connected to the SourceMeter 4W Sense HI via relay pins 11 and 3. Point C is connected to SourceMeter 4W sense LO via pins 12 and 4 and lastly, point D of the sample is connected to the SourceMeter I/O LO. These connections makes current to be sourced via the points A and D and voltage drop in the sample measured across the points B and C.

When the relay was switched ON by the computer's printer port, the relay contacts as above were disabled and new contacts made. Now, point A was connected to the computer I/O HI via relay pins 9 and 5 and point B connected to the unit I/O LO via relay pins 11 and 7. Point C was connected to the unit 4W Sense LO via the relay pins 12 and 8 and lastly, sample point D was connected to the unit 4W Sense HI via the relay pins 10 and 6. These new contacts now made the current to be sourced to the sample at the points A and B and corresponding voltages measured via the points D and C.

4.7.3 Measurements of Voltage and Current by Keithley SourceMeter

The SourceMeter was used to perform both sourcing and measuring (sensing) at the same time. In order to minimize errors in readings due to potential drops in the test leads when sourcing or reading voltages, the four wire remote sensing operation was adopted. When sourcing voltage, 4-wire remote sensing ensured that the programmed voltage was delivered to the thin film under test. The 4-W connection is as depicted in figure 4.15

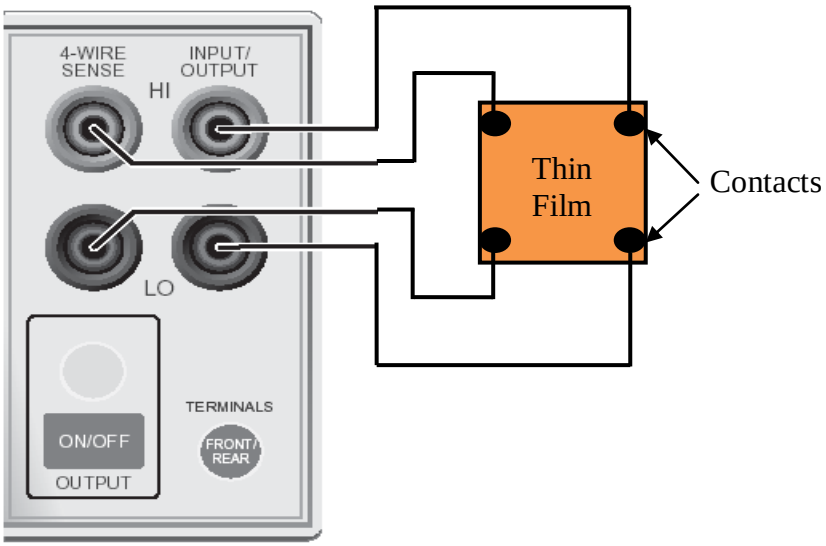

Fig.4.15: Keithley SourceMeter four-wire remote sensing connections (Keithley Instruments, 1998)

Other SMU capabilities that were used are: sweep operations, concurrent measurements and remote interfaces (RS-232C).

Once the connection between the thin film sample, the switching device and SMU were done and serial communication between the computer and the latter verified, there was need to have full control of the SMU. This required the use of Ke24xx VIs. After initializing the instrument using Ke24xx Initialize.vi, the following VISA VIs were used for full control of the instrument:

(i) Ke24xx Configure Source Mode.vi

(ii) Ke24xx Configure Source Sweep.vi

(iii) Ke24xx Configure Source Compliance.vi

(iv) Ke24xx Select Sense Functions.vi

(v) Ke24xx Enable/Disable Remote Sensing.vi

(vi) Ke24xx Enable/Disable Concurrent Meas.vi

(vii) Ke24xx Configure DCV.vi

(viii) Ke24xx Configure DCI.vi

(ix) Ke24xx Configure Trigger Layer.vi

(x) Ke24xx Configure Buffer.vi

(xi) Ke24xx Enable/Disable Buffer.vi

(xii) Ke24xx Enable/Disable Source Output.vi

(xiii) Ke24xx Read Buffer.vi

(xiv) Ke24xx Close.vi

4.7.3.1 Ke24xx Configure Source Mode.vi

This VI was used to configure the source mode of the Keithley SourceMeter instrument. It's controls function and mode were set at current and sweep respectively as shown on the block diagram below. With current (1) function selected, it ensured that the instrument sourced current to the semiconductor sample. The mode function selected the waveform type for the source function. The sweep function (linear staircase) was the selected mode as depicted in the code below.

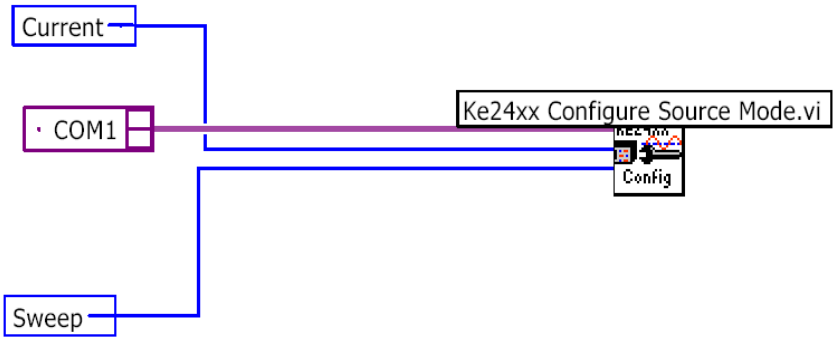

Fig. 4.16: Ke24xx Configure Source Mode.vi block diagram

4.7.3.2 Ke24xx Configure Source Sweep.vi

This VI was used to set the value of current to be sourced. The controls to this VI were set as depicted in table 4.3.

Table 4.3: Settings to configure source sweep operation in the SourceMeter

Spacing	Linear staircase
Ranging	Best
Start value	1E-10
Stop value	1E-10
Number of points	50

These settings are as shown in the block diagram code in figure 4.17.

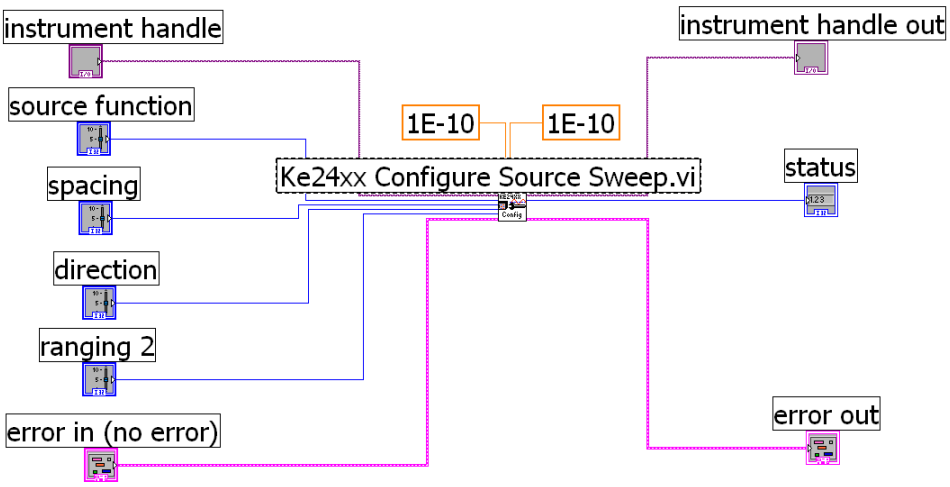

Fig. 4.17: Block diagram code to configure source sweep operation

With linear staircase mode, this function made the current to go from the start level (1E-10 A) to top level (1E-10 A) in fifty equal linear steps. This was done in order for the instrument to source the same amount of current to the sample fifty times and measure the corresponding voltage. The mean current and mean voltages were then calculated using mean.vi to minimize errors in these measurements. These averages were later used for sheet resistivity computation. Figure 4.18 shows a schematic of linear staircase sweep mode operation comprising of five steps.

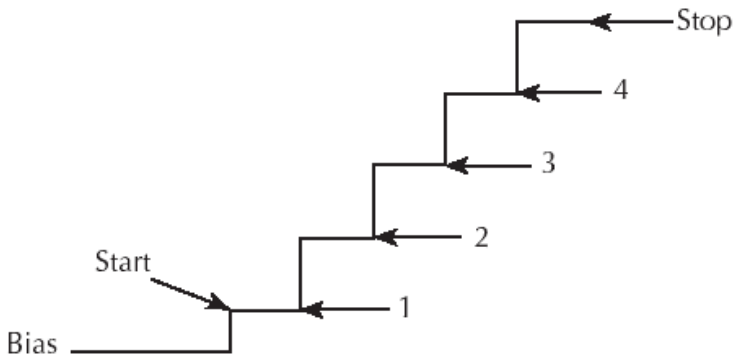

Fig. 4.18: A schematic of linear staircase sweep mode operation

4.7.3.3 Ke24xx Configure Source Compliance.vi

This function was used to set the maximum compliance value for both sense functions (DCI and DCV). This was set at 100 mV. The measured voltage could not exceed this set compliance limit. The block diagram code in figure 4.19 was used to configure source compliance.

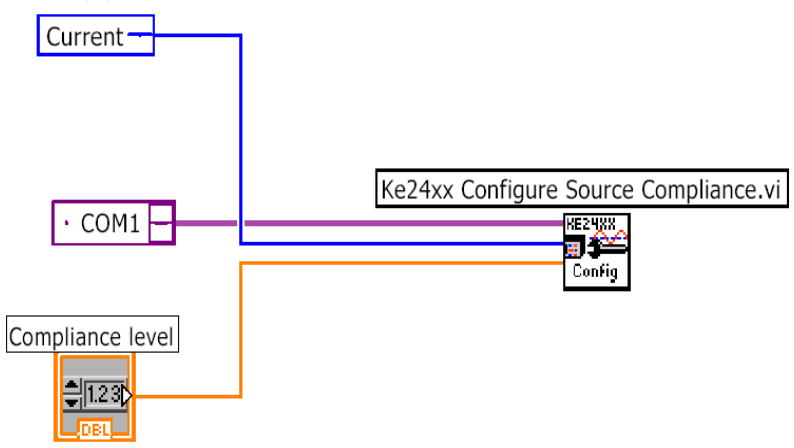

Fig. 4.19: Ke24xx Configure Source Compliance.vi block diagram

4.7.3.4 Ke24xx Select Sense Functions.vi

This function was used to select functions to be measured by the SourceMeter by assigning Boolean controls to them. Both *dci* and *dcv* controls were assigned Boolean true (T) while *res* was assigned Boolean false (F) as shown in figure 4.20. This was because only the voltage drops across the sample were to be measured.

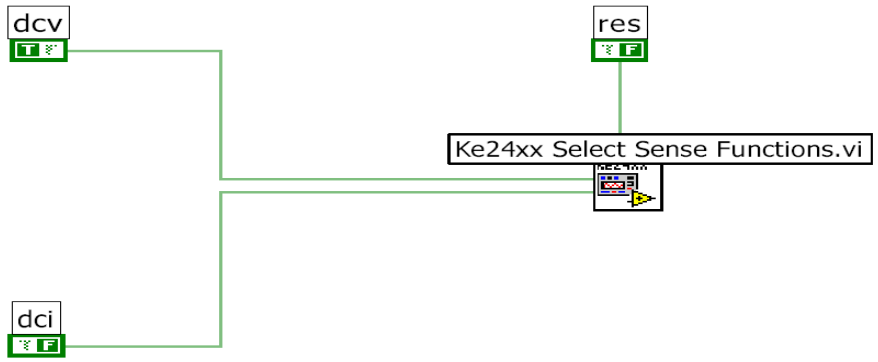

Fig. 4.20: Ke24xx Select Sense Functions.vi block diagram code

4.7.3.5 Ke24xx Enable/Disable Remote Sensing.vi

This function was used to control the remote sensing (2-W or 4-W sensing). Remote sensing was activated by assigning a Boolean true (T) to the state controls as shown in figure 4.21. This was to ensure that the SourceMeter unit is controlled remotely (using a remote computer) as opposed to local control.

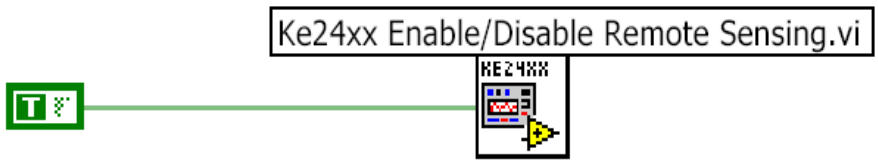

Fig. 4.21: Ke24xx Enable/Disable Remote Sensing.vi block diagram code

4.7.3.6 Ke24xx Enable/Disable Concurrent Meas.vi

This function was used to enable concurrent measurement on both DCV and DCI by the SourceMeter unit. The state control to this function was set at Boolean true (T) as depicted in figure 4.22. Both the sourced current and the corresponding voltages were measured and stored in the instrument's buffer and later used for sheet resistivity computation.

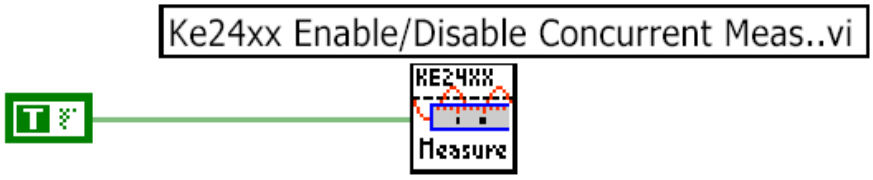

Fig. 4.22: Ke24xx Enable/Disable Concurrent Meas.vi block diagram code

4.7.3.7 Ke24xx Configure DCV.vi

The function was used to set up the DCV (Direct Current Voltage) sense function. The range was set at *auto* and NPLC (Number of power line cycles) at 1.00E+0 as shown in a block diagram code of figure 4.23.

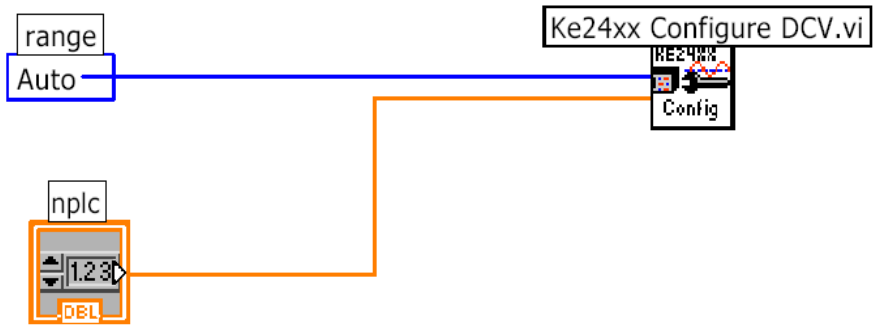

Fig. 4.23: Ke24xx Configure DCV.vi block diagram

4.7.3.8 Ke24xx Configure DCI.vi

The function was used to set up the DCV (DC Voltage) sense function. The range was set at *auto* so that the best measurement range could be automatically selected. The NPLC (Number of power line cycles) was set at 1.00E+0. This is a compromise between the speed and noise in the measurements. The figure below shows the above settings.

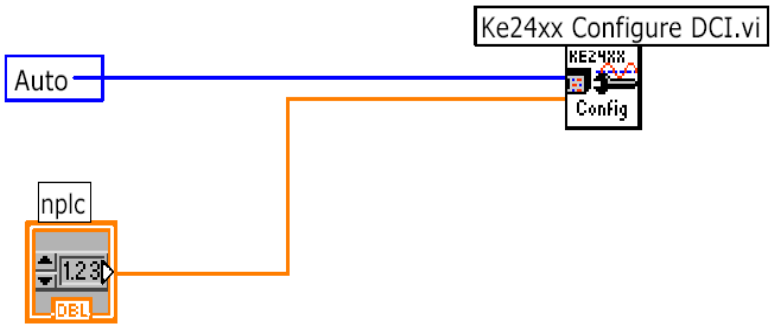

Fig. 4.24: Ke24xx Configure DCI.vi block diagram code

4.7.3.9 Ke24xx Configure Trigger Layer.vi

The function was used to set up trigger layer of the SourceMeter trigger model. The trigger delay determined the time in milliseconds set for the instrument to be triggered to start operation. This was set at 0.00E+0 (zero) so that the unit operation was immediate when the program was run. The count was set at 50 as shown in the figure 4.25 so that the SMU could be triggered fifty times in each sequence.

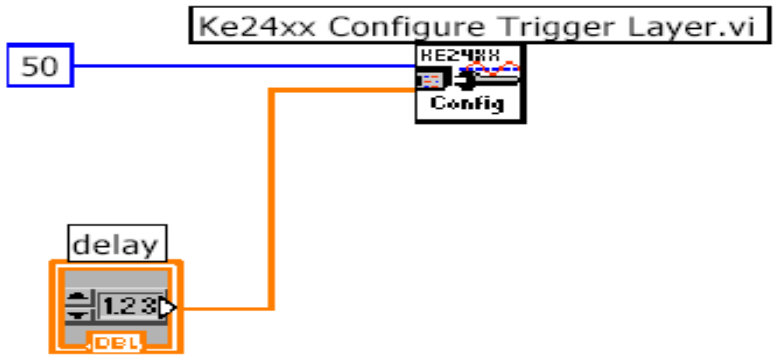

Fig. 4.25: Ke24xx Configure Trigger Layer.vi block diagram code

4.7.3.10 Ke24xx Configure Buffer.vi

The function was used to control the buffer size of the SourceMeter. These are storage locations for the measurements done. Since fifty measurements were required for each sequence, buffer size was set at 50 as depicted in the code below.

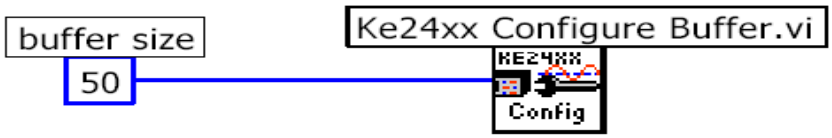

Fig. 4.26: Ke24xx Configure Buffer.vi block diagram code

4.7.3.11 Ke24xx Enable/Disable Buffer.vi

This is another function used to set up the SourceMeter buffer content. When this VI was activated, the measured values were stored in its buffer. It was enabled by keeping the status control of the VI at Boolean true (T) as shown in figure 4.27.

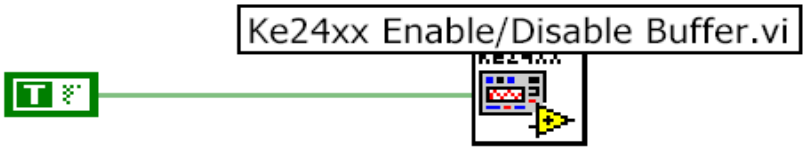

Fig. 4.27: Ke24xx Enable/Disable Buffer.vi

4.7.3.12 Ke24xx Enable/Disable Source Output.vi

By keeping the status control of this function at Boolean True (T) as shown in figure 4.28, the source output (current) was enabled. This function ensured that the sourced current was output by the SMU and stored in its buffer.

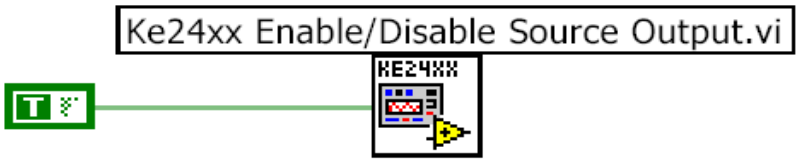

Fig. 4.28: Ke24xx Enable/Disable Source Output.vi block diagram code

4.7.3.13 Ke24xx Read Buffer.vi

This function was used to obtain the readings from the instrument's buffer. The block diagram below shows how the measured voltage values were read from these storage locations by setting the elements control at 1.

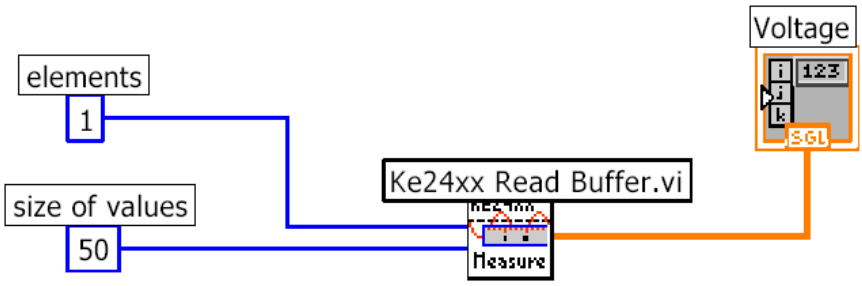

Fig. 4.29: Ke24xx Read Buffer.vi block diagram code to read voltage

In order to read current values from the buffer, the elements control for the VI was set at 2 as depicted in the block diagram code below.

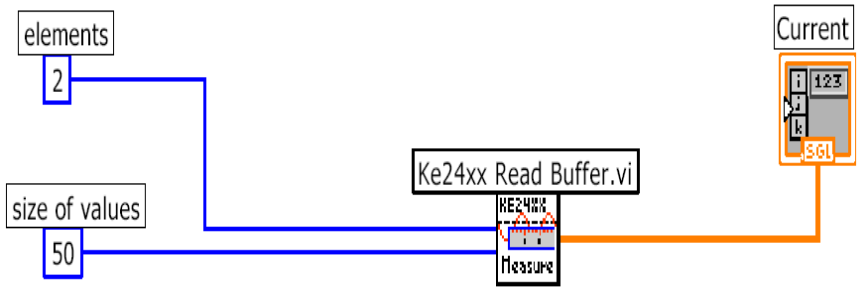

Fig. 4.30: Ke24xx Read Buffer.vi block diagram code to read current

4.7.3.14 Ke24xx Close.vi

The function was used to perform closing the instrument's session. This ensured that the SourceMeter could not be used further unless it was re-initialized. Figure 4.31 depicts Ke24xx Close.vi.

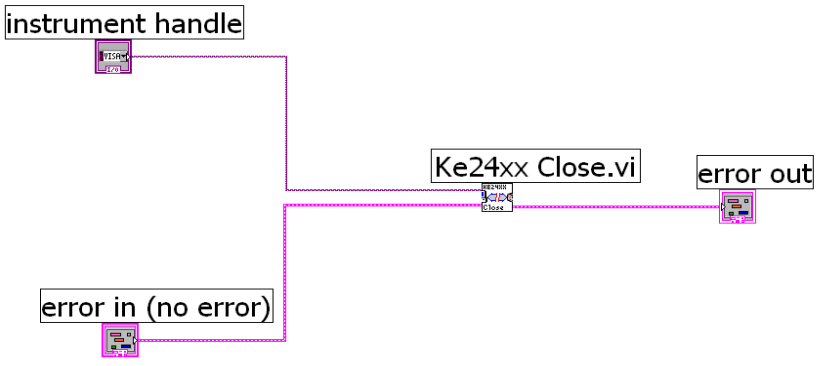

Fig. 4.31: Ke24xx Close.vi block diagram code

All these VIs were wired together to form a whole code for full instrument (SourceMeter) control as shown in the block diagram code in figure 4.33.

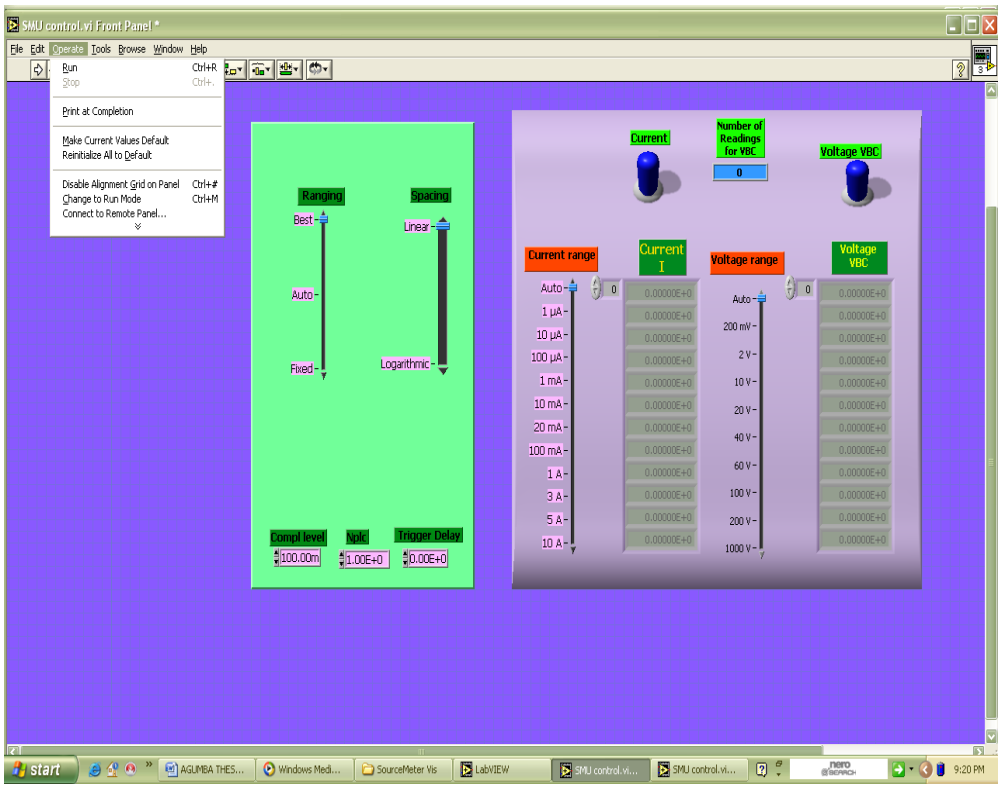

Fig. 4.32: Full SourceMeter control Front panel VI

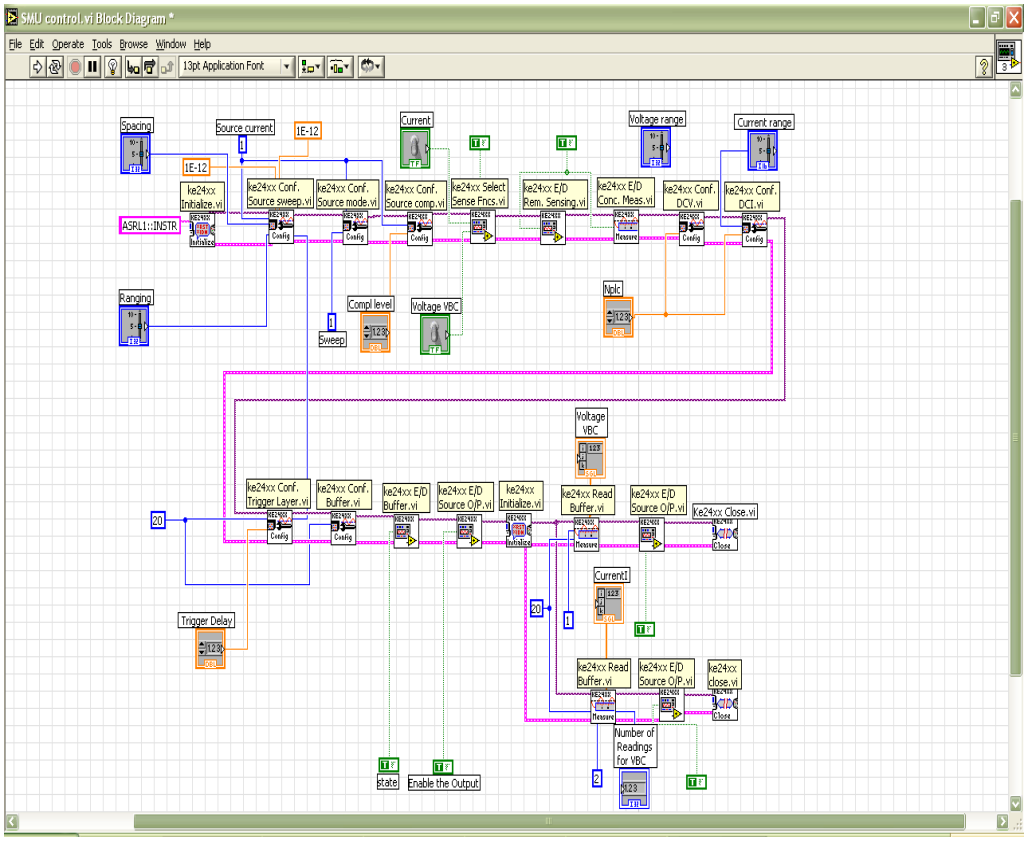

Fig. 4.33: Full SourceMeter control block diagram code

When the program was run by clicking the run button or Ctrl+R buttons, the SourceMeter unit was initialized and set for measurements. The unit then checked if the intended readings were in compliance with the compliance level set at 100 mV. This compliance level was indicated on the SMU screen. A star on the unit screen indicated that the buffer was enabled and ready for storage of the sourced and read data. The SourceMeter then made array of fifty measurements of sourced current and corresponding sensed voltages when the switching device was in OFF state. In the next sequence structure when the switching device was in ON state, fifty current and voltage values were sourced and read respectively before the switching device was turned OFF in the second sequence

structure. These measurements were read from the unit buffer by use of Ke24xx read from buffer.vi and sent to the computer which made them available for sheet resistivity computation. After the measurement was done, the Ke24xx close.vi ended the session and the SourceMeter unit was set to default idle mode.

4.7.4 Thin Film Sheet Resistivity Computation

From the Van der Pauw set-up equation with probing done twice, the variables required for sheet resistivity computation were sourced current *I*, sensed voltages V_{BC} and V_{DC} and the film thickness *t*. The stacked sequence structure was used to trigger the SMU and the Van der Pauw switching device in a sequence in order to measure V_{BC} and V_{DC} respectively. In the initial stacked sequence structure 0[0..1], current was sourced through the tips AD and array of voltage V_{BC} measured between the probe tips B and C with the Van der Pauw switching circuit OFF. Figure 4.34 shows the block diagram code for the first stacked sequence code.

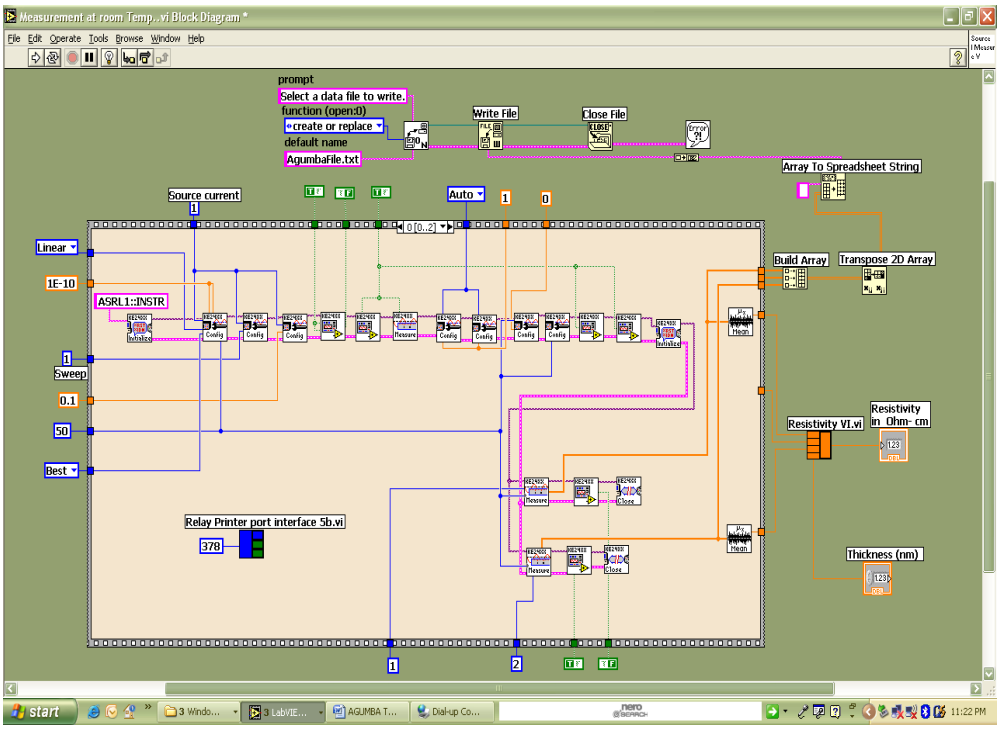

Fig. 4.34: Block diagram showing the first sequence code for V_{BC} sensing

In the second stacked sequence structure 1[0..1], current was now sourced through the probe tips AB and array of voltage V_{DC} measured between the probe tips D and C. This switching was done by use of the designed Van der Pauw switching device which was activated in this part of the code. Figure 4.35 shows the second stacked sequence code.

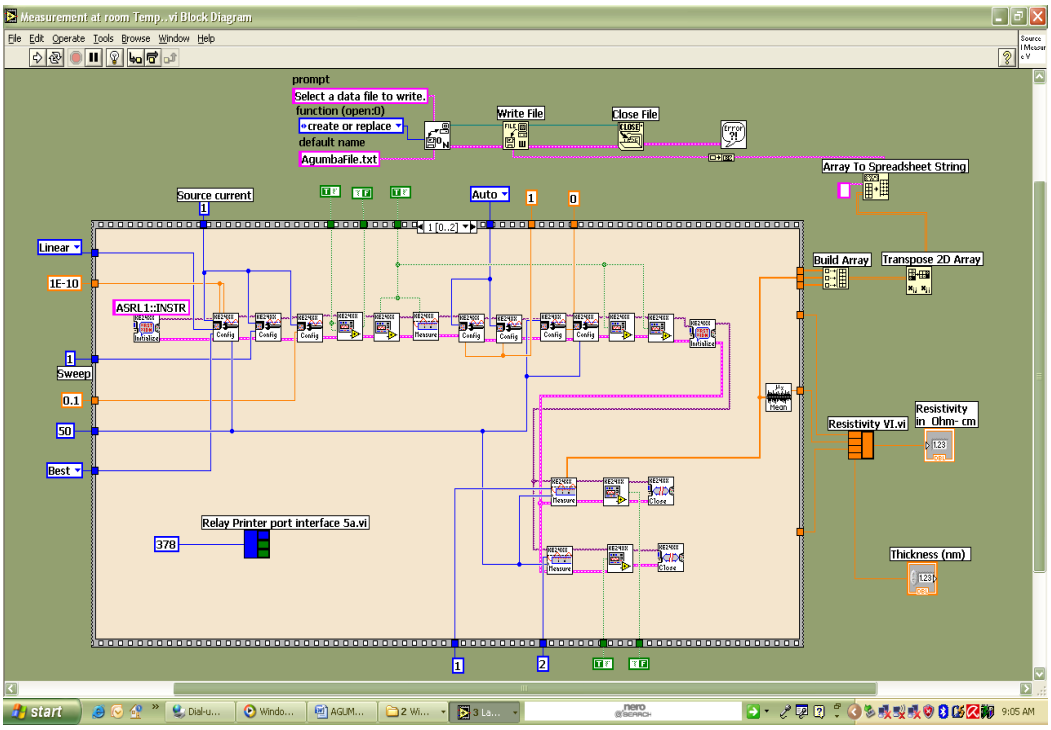

Fig. 4.35: Block diagram showing the second sequence code for V_{DC} sensing

The third stacked sequence structure contained a sub-VI to turn off the Van der Pauw switching device and return it to its initial OFF mode as depicted in figure 4.36.

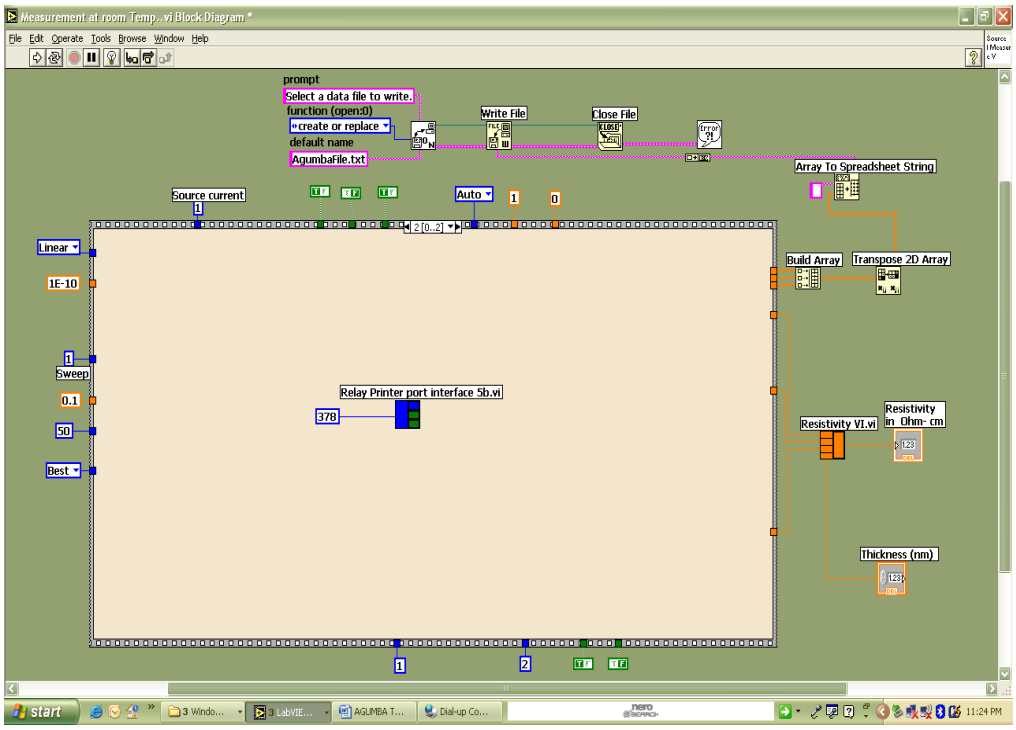

Fig. 4.36: Block diagram showing the third sequence code to turn OFF the switching device

Once the arrays of current and voltages V_{BC} and V_{DC} were measured by the SourceMeter unit and displayed on the computer, their mean were obtained by use of mean.vi. These values were forwarded to sheet resistivity sub-VI for computation of sheet resistivity.

Considering the sheet resistivity equation 3.31, a number of sub-VIs were required for sheet resistivity computation. These sub-VIs are analogous to subroutines in text-based languages and are recalled for sheet resistivity computation whenever they are required. The four sub-VIs required for computation of this parameter are outlined below.

(i) Correction factor VI (Q VI.vi)

(ii) Correction factor to symmetry factor VI (Q to F VI.vi)

(iii) Sheet resistance VI.vi

(iv) Resistivity VI.vi

4.7.4.1 Correction factor VI (Q VI.vi)

This sub-VI computed the equation 3.28. The sub-VI compared the input voltages V_{BC} and V_{DC} and output the value of Q. This was accomplished by use of case structure where exactly only one structure executed when the value wired to its inputs satisfied the conditions for the structure execution. The user interface (Front panel) in figure 4.37 displays the value of Q determined that was later called when Q to F sub-VI was executed. The corresponding block diagram code is depicted in figure 4.38.

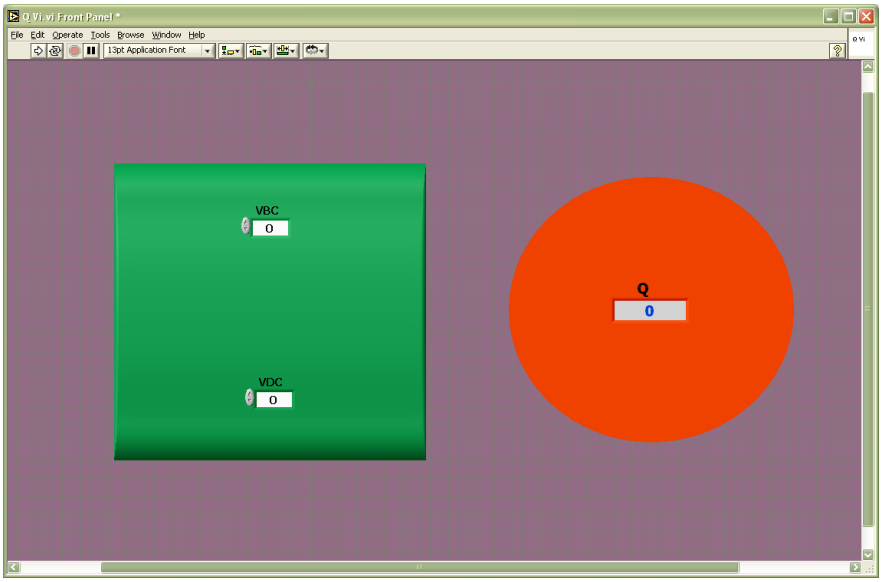

Fig.4.37: Front panel of Q VI.vi for computing correction factor Q

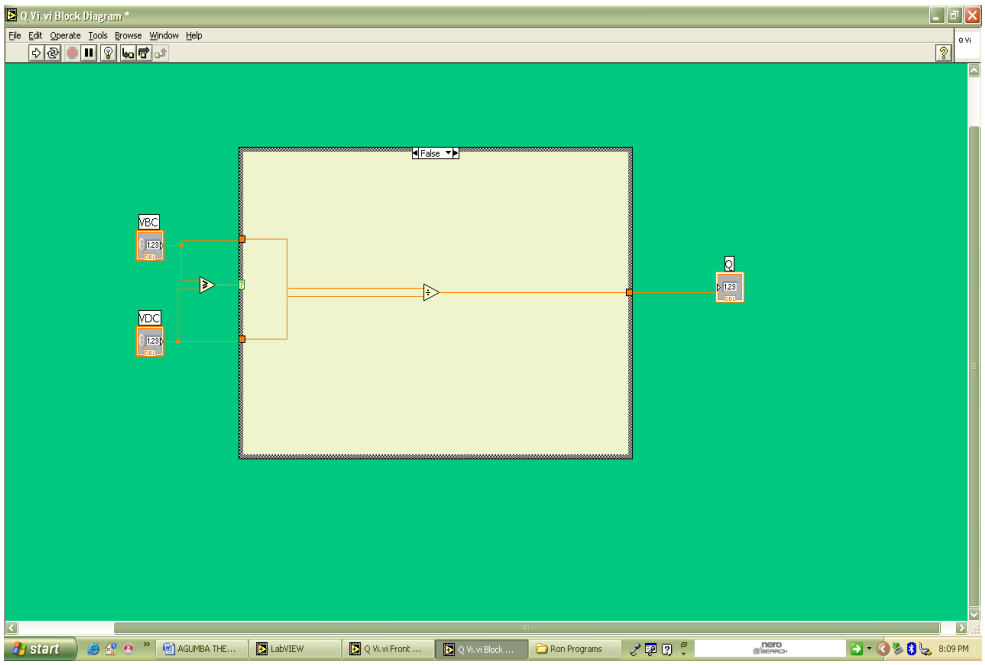

Fig. 4.38: Block diagram code for Q VI.vi to compute correction factor Q

4.7.4.2 Correction factor to symmetry factor VI (Q to F.vi)

This sub-VI computed the equation 3.29 by calling the correction factor Q VI.vi worked above. The front panel in figure 4.39 shows the output *F* which was later called when the sheet resistance VI was executed and the actual code is shown in figure 4.40.

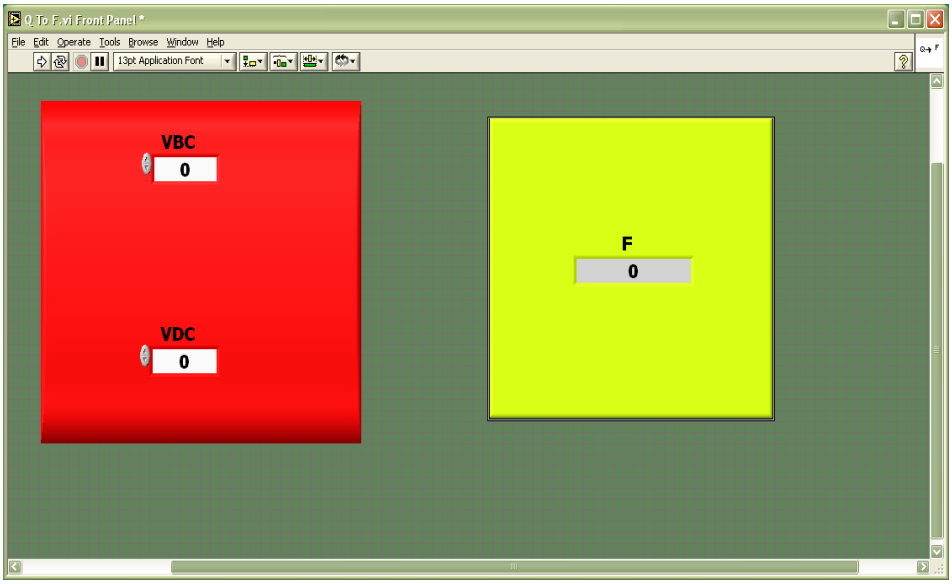

Fig. 4.39: Front panel of Q to F VI.vi for computing symmetry factor, F from correction factor, Q

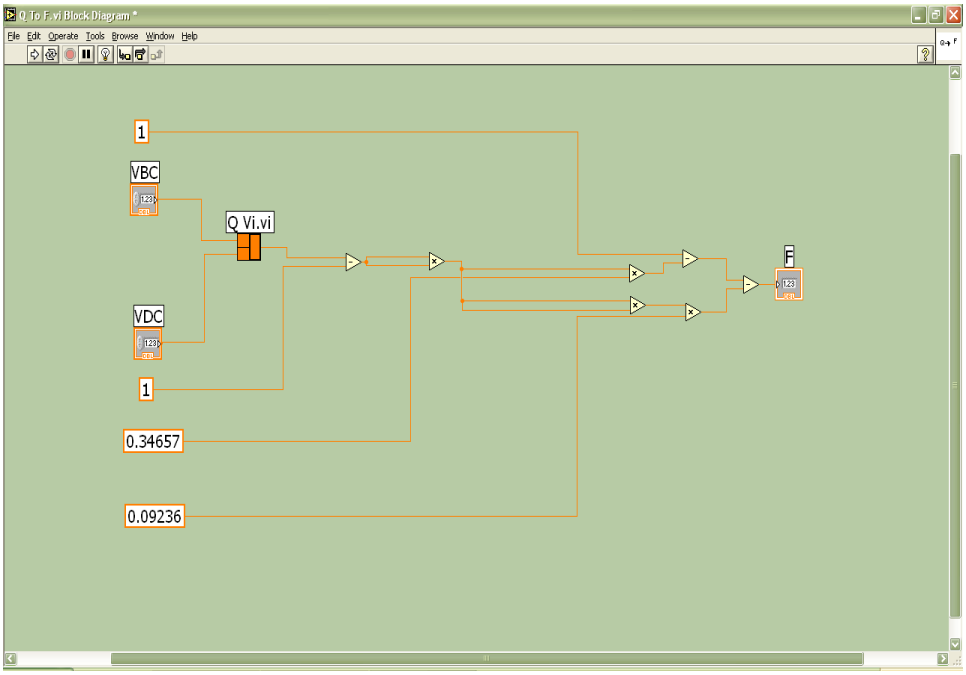

Fig. 4.40: Block diagram code of Q to F VI.vi for computing symmetry factor, F from correction factor, Q

4.7.4.3 Sheet Resistance .vi

This sub-VI was used to compute the equation 3.27 by making use of the constants π and ln2, the variables V_{BC}, V_{DC} and current *I*. The F to Q sub-VI was also called for this computation. The sheet resistance sub-VI front panel and block diagram codes are shown in figures 4.41 and 4.42 respectively.

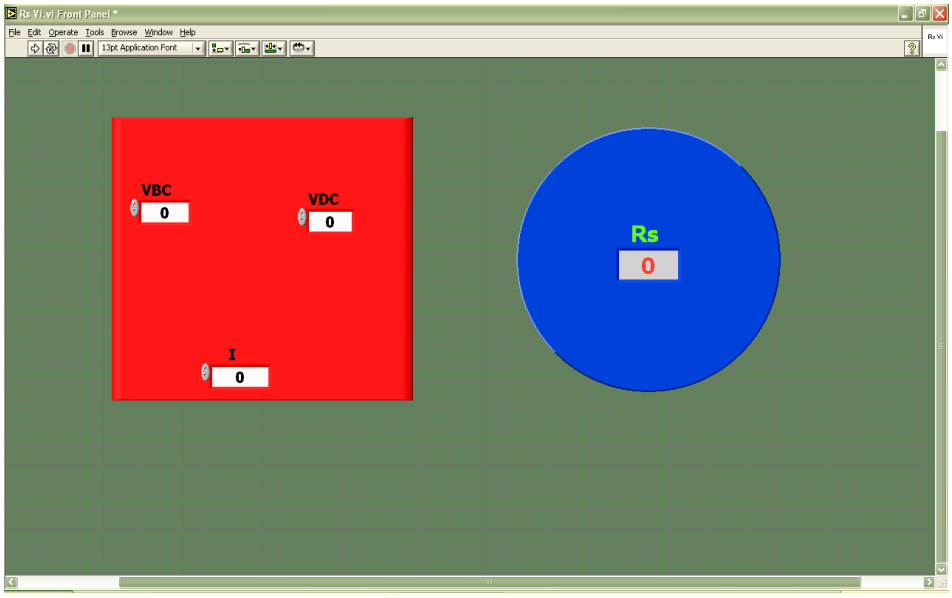

Fig.4.41: Front panel of Sheet Resistance VI.vi for computing sheet resistance

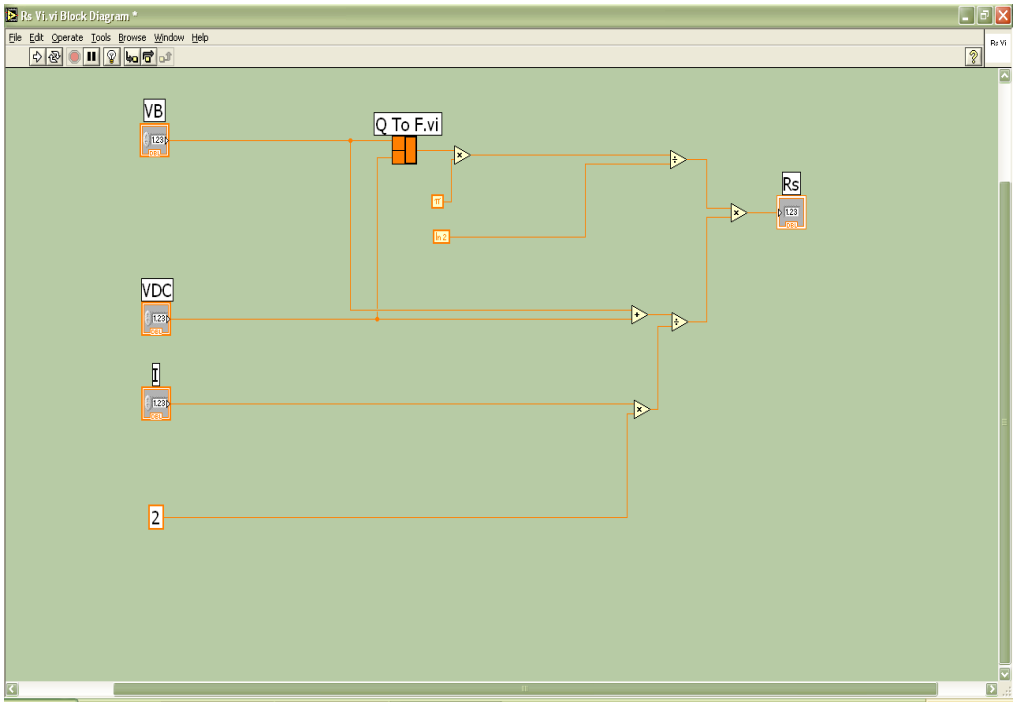

Fig. 4.42: Block diagram code of Sheet Resistance VI.vi for computing sheet resistance

4.7.4.4 Sheet Resistivity .vi

Lastly, this Sub-VI yielded sheet resistivity by computing the equation 3.31 by making use of the film thickness (*t*) in nanometers obtained by profilometry method. Multiplication by 100 was to make the sheet resistivity be computed in ohm-cm rather than ohm-metre.

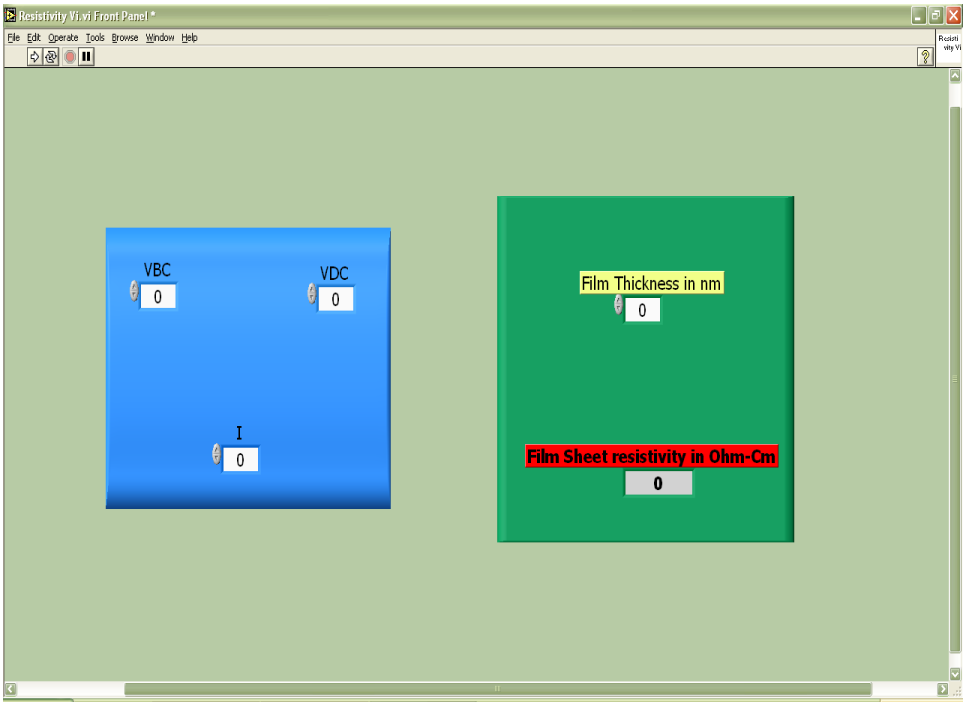

Fig. 4.43: Front panel of Sheet Resistivity VI.vi for sheet resistivity computation

Figure 4.43 was used to display the sheet resistivity after computation. With V_{BC}, V_{DC}, I and film thickness t made available to the controls of this sub-VI, the sheet resistivity was computed and displayed in the front panel. The block diagram in figure 4.44 depicts the actual code for the computation of thin film sheet resistivity.

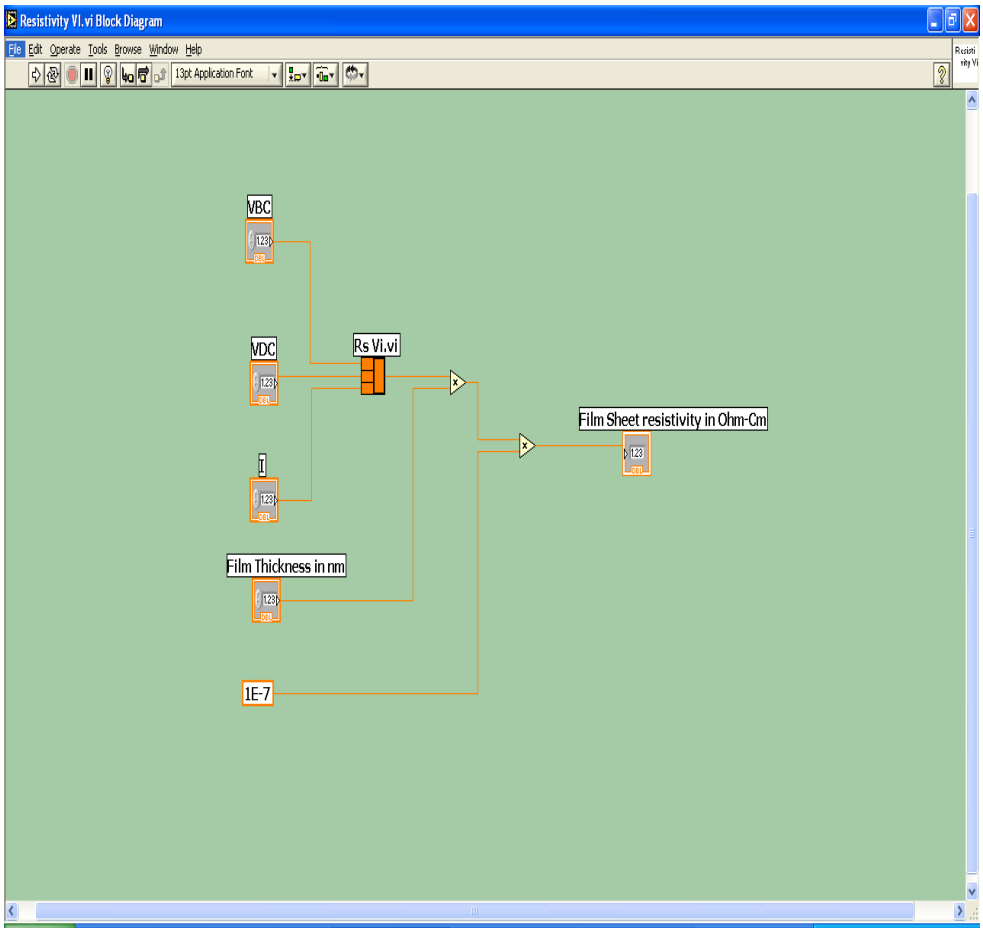

Fig. 4.44: Block diagram code of Sheet Resistivity VI.vi for sheet resistivity computation

CHAPTER FIVE

RESULTS AND DISCUSSIONS

5.1 Four Point Probe Head Design and Fabrication

The probe head was successfully designed and fabricated from easily available materials. The four probe tips were contained on a perspex mechanical stage that moved up and down from and to a stage on which the film sample whose resistivity was to be measured was mounted. Aluminum rods were used as the probe tips. However, platinum rods were the most ideal for there to be ohmic contact between the probe tips and the semiconductor thin films surface. The use of aluminum for probe tips introduced a small level of schottky barrier between their tips and the thin film sample.

5.2 Switching Device Design and Fabrication

A computer controlled relay switching device designed and fabricated performed the Van der Pauw switching on the thin film sample well. The switching of the transistor ON and OFF was accomplished by LabVIEW software that controlled the computer printer port on which the interfacing was done. Having been controlled by the computer printer port, the switching transistor controlled the switching of the relay. With the use of 14 pin relay, the switching of the four probe tips on the sample surface was done without physically changing their initial positions. This avoided the damage of the thin film surface due to scratch and also reduced errors due to change in symmetry.

5.3 Interfacing of Keithley SourceMeter

Full remote SourceMeter control was achieved by interfacing it to a computer via the serial (RS-232) port. A LabVIEW programming environment was used to achieve this control. The computer initialized the SMU, configured it, triggered it, measured and saved the readings of sourced current and sensed voltage in the SMU buffer. The interfacing was achieved by use of VISA VIs. There was first the installation of Keithley 24xx PnP instrument driver available at the National Instruments website into a LabVIEW running computer. The instrument driver is in a package of VISA VIs that are used for easy building of the VIs for controlling the Keithley device without going into the intricacies of lower level programming. The use of these VIs helped to save the programs development time with a great factor.

5.4 Interfacing of the Relay Switching Device

Once the Van der Pauw switching device was designed and developed, it was controlled remotely by a computer via its LPT1 port. The interface was achieved by use of inport.vi and outport.vi available at the functions palette. The Van der Pauw switching device was fully controlled by the computer. The ON and OFF states were achieved by use of sequence structures. In the initial sequence structure, V_{BC} was measured with the switching device in OFF mode. In the first sequence structure when V_{DC} was measured, the switching device was in ON state. In the last sequence structure, the switching device was returned to its default OFF state.

5.5 The Test Sample Sheet Resistivity Measurement at Room Temperature

The developed probe head, Van der Pauw switching device, SourceMeter 2400 and a LabVIEW running computer combination were first used for sheet resistivity measurement of the test sample prepared at given sputtering conditions. LabVIEW VIs were developed to fully control the SMU device for measurements of voltage and current across the test sample which were later used for sheet resistivity computation. Figure 5.1 shows a full code for sheet resistivity measurement.

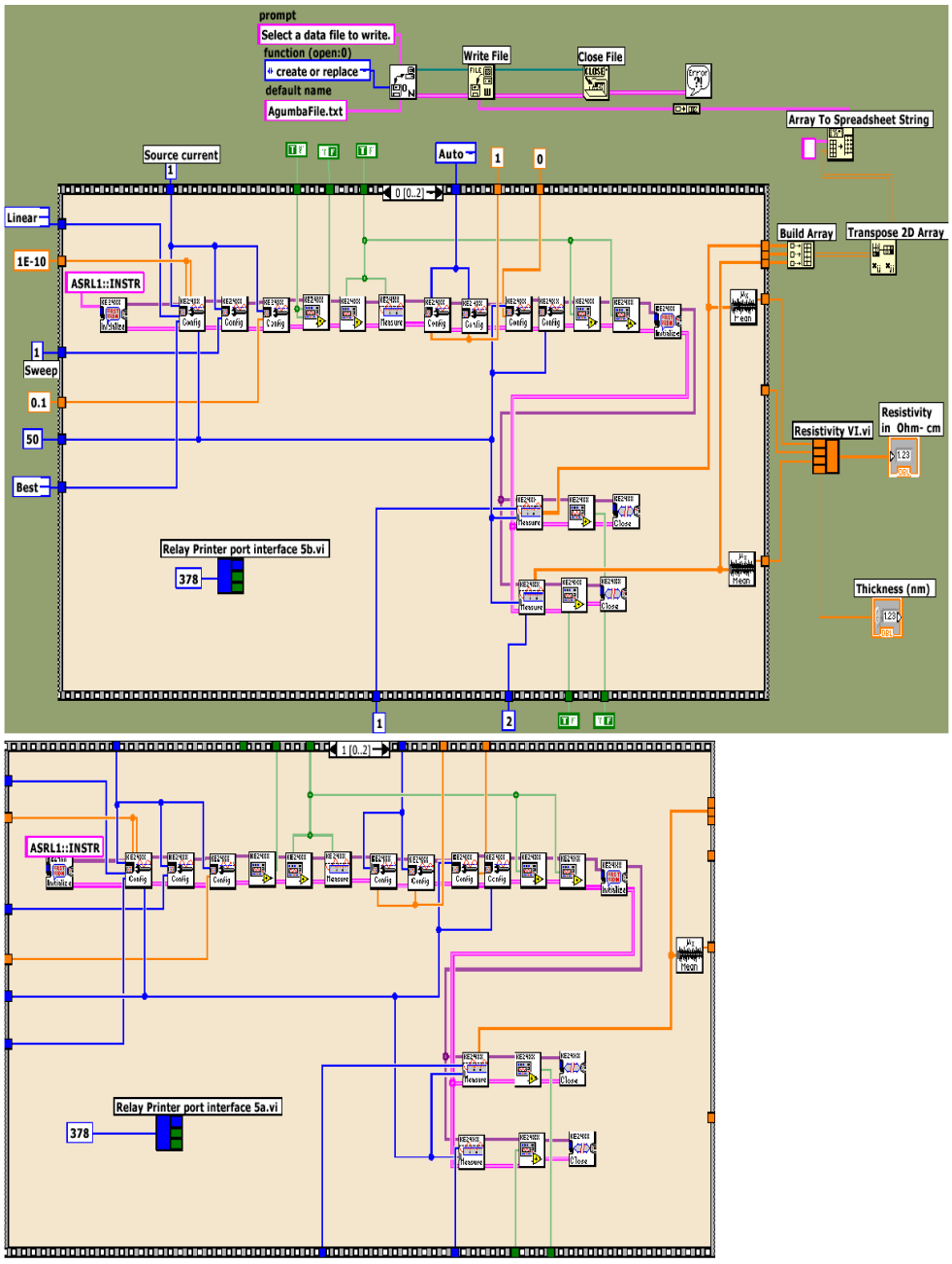
prompt
Select a data file to write.
function (open:0)
create or replace
default name
AgumbaFile.txt
Write File
Close File
Array To Spreadsheet String
Source current
Auto
Linear
1E-10
ASRL1::INSTR
Sweep
0.1
50
Best
Build Array
Transpose 2D Array
Resistivity VI.vi
Resistivity in Ohm- cm
Thickness (nm)
Relay Printer port interface 5b.vi
378
Relay Printer port interface 5a.vi

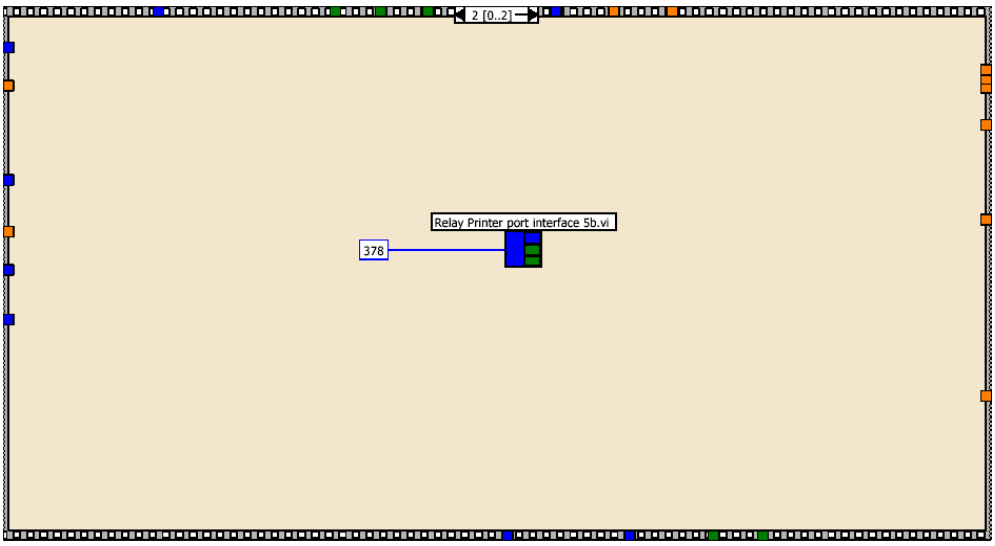

Fig. 5.1: Full block diagram codes to perform sheet resistivity measurement

The front panel in figure 5.2 shows the user GUI where the film thickness in nanometers is entered and the sheet resistivity is directly read when the program is executed.

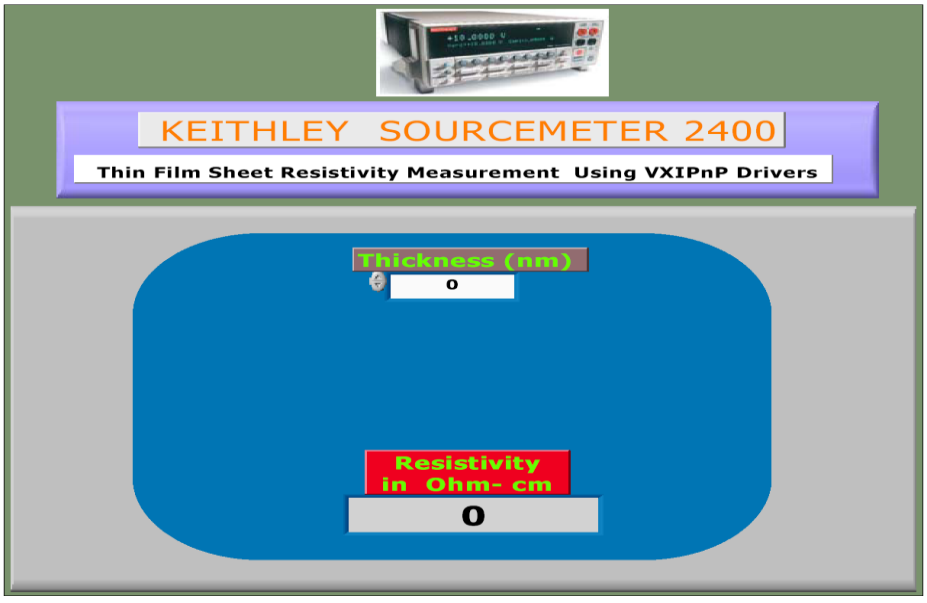

Fig. 5.2: Front Panel (GUI) for sheet resistivity measurement

When the program was executed, the SMU was initialized, triggered and performed current and voltage sweeps across the sample. Equal amount of current (1×10^{-10} A) was sourced into the sample fifty times when the switching device was in OFF state and corresponding voltage measured. These represented the current sourced through pins A and D (I_{AD}) and voltage drops across the pins B and C (V_{BC}). When the switching device was in ON state, the same amount of current was now sourced through the pins A and B (I_{AB}) fifty times and corresponding voltage drops across pins C and D (I_{DC}) was measured. Table 5.1 shows the sourced current *I*, measured voltage drops across the test sample V_{BC} and V_{DC} respectively.

Table 5.1: Sourced current I, measured voltages V_{BC} and V_{DC} across the test sample

Measured Voltage (V_{BC})	Measured Voltage (V_{DC})	Sourced current (I)
0.000164	0.000162	1.324760E-10
0.000161	0.000164	1.324759E-10
0.000163	0.000162	1.324760E-10
0.000163	0.000162	1.324339E-10
0.000162	0.000163	1.325181E-10
0.000164	0.000164	1.325601E-10
0.000162	0.000164	1.329388E-10
0.000162	0.000163	1.325601E-10

Table 5.1 continued

0.000163	0.000162	1.318448E-10
0.000162	0.000163	1.324339E-10
0.000163	0.000164	1.323077E-10
0.000162	0.000164	1.326443E-10
0.000162	0.000163	1.326443E-10
0.000163	0.000164	1.321393E-10
0.000163	0.000163	1.328127E-10
0.000162	0.000165	1.326863E-10
0.000162	0.000163	1.327283E-10
0.000162	0.000162	1.326443E-10
0.000161	0.000164	1.327705E-10
0.000163	0.000163	1.325179E-10
0.000161	0.000163	1.325180E-10
0.000161	0.000162	1.327705E-10
0.000163	0.000162	1.328547E-10
0.000161	0.000165	1.325180E-10
0.000162	0.000160	1.326864E-10
0.000163	0.000165	1.322235E-10

Table 5.1 continued

0.000162	0.000163	1.323497E-10
0.000162	0.000163	1.321394E-10
0.000163	0.000164	1.328125E-10
0.000161	0.000163	1.324760E-10
0.000163	0.000164	1.323917E-10
0.000163	0.000163	1.327283E-10
0.000163	0.000163	1.326021E-10
0.000163	0.000162	1.325180E-10
0.000161	0.000163	1.324338E-10
0.000162	0.000163	1.325180E-10
0.000163	0.000164	1.327704E-10
0.000162	0.000163	1.328967E-10
0.000163	0.000162	1.326863E-10
0.000164	0.000163	1.324760E-10
0.000162	0.000165	1.323077E-10
0.000163	0.000163	1.318868E-10
0.000163	0.000163	1.322235E-10
0.000161	0.000163	1.324759E-10

Table 5.1 continued

0.000163	0.000163	1.323497E-10
0.000162	0.000163	1.330650E-10
0.000162	0.000165	1.325601E-10
0.000164	0.000163	1.323077E-10
0.000161	0.000162	1.323076E-10
0.000162	0.000163	1.325180E-10

After the measurements of voltage and current values and their averages obtained as depicted in table 5.2, these parameters together with the thin film sample's thickness were fed into sheet resistivity.vi for sheet resistivity computation as depicted in the front panel in figure 5.3.

Table 5.2: Mean V_{BC}, V_{DC} and I

Mean V_{BC} (V)	Mean V_{DC} (V)	Mean I (A)
$1.62x10^{-4}$	$1.63x10^{-4}$	$1.3260x10^{-10}$

From the above measurements, the test sample of thickness 99.27 nm was found to have a sheet resistivity of **55.6548 Ω cm** as shown in the front panel below.

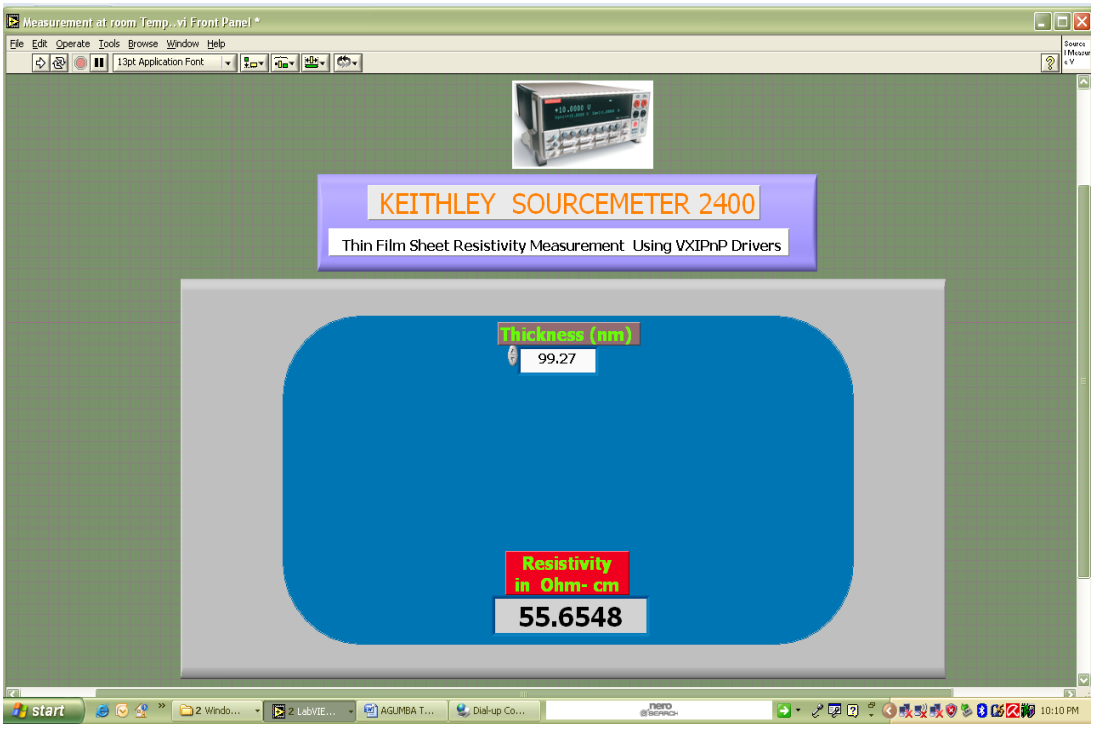

Fig. 5.3: Front panel showing the display of sheet resistivity measured

5.6 The Test Thin Film Sample Sheet Resistivity at Various Temperatures

The sheet resistivity of the test sample measured at varied temperatures of 23 ^{o}C, 27 ^{o}C, 45 ^{o}C, 55 ^{o}C, 70 ^{o}C, 90 ^{o}C, 100 ^{o}C, 120 ^{o}C, 145 ^{o}C and 170 ^{o}C carried out in an electric furnace (Lindberg/Blue) gave the results as shown in table 5.3.

Table 5.3: Test sample sheet resistivity at different temperatures

Temperature (^oC)	V_{BC} ($x10^{-4}V$)	V_{DC} ($x10^{-4}V$)	I (A)	Sheet resistivity (Ω cm)
23	1.706	1.790	$1.435x10^{-10}$	55.0837
27	1.405	1.391	$1.324x10^{-10}$	47.9104
45	1.287	1.470	$1.337x10^{-10}$	46.4209
55	1.294	1.296	$1.321x10^{-10}$	44.4033
70	1.279	1.306	$1.325x10^{-10}$	44.2000
90	1.280	1.249	$1.323x10^{-10}$	43.3235
100	1.232	1.175	$1.325x10^{-10}$	41.1438
120	1.208	1.093	$1.328x10^{-10}$	39.0936
145	0.969	1.071	$1.335x10^{-10}$	34.5055
170	0.914	0.814	$1.354x10^{-10}$	29.6691

When sheet resistivity of the thin film was plotted as a function of temperature, the graph in figure 5.4 was obtained. As depicted in the graph, it is seen that the surface sheet resistivity at room temperature of 23 ^oC was 55.0837 Ω cm. As the sample temperature was increased above room temperature, the sheet resistivity dropped and was at its minimum value of 29.6691 Ω cm at a temperature of 170 ^oC.

Fig. 5.4: Graph of film Sheet Resistivity (Ω cm) versus Film Temperature (^{o}C)

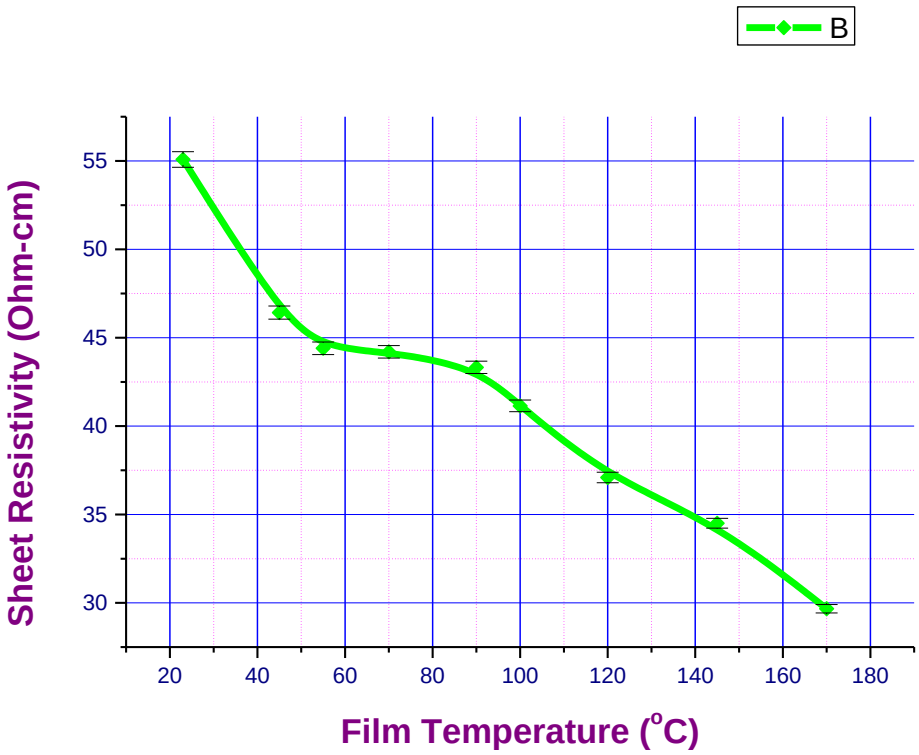

Crystal defects could result during the thin film deposition and the drop in sheet resistivity from 55.0837 Ω cm to 29.6691 Ω cm with temperature rise from room of 23 ^{o}C to temperature of 170 ^{o}C could be attributed to healing of these crystal defects. Again, high film sheet resistivity at room temperature could be attributed to polycrystalline phases of Cu, Cu_2O and CuO present in the film. High temperatures increased the crystallinity of the film with a single phase of Cu_2O of higher carrier mobility formed. These values of sheet resistivity measured at different temperatures agree with experimental results of Onimisi, 2008 with the confirmation that this parameter drops with increase in film temperature.

5.7 Variation of Cu_2O Sheet Resistivity with Sputtering Pressure

The table below shows the sheet resistivities of seven samples prepared at sputtering pressures of 1.8 Pa, 1.9 Pa, 2.0 Pa, 2.1 Pa, 2.2 Pa, 2.3 Pa and 2.4 Pa.

Table 5.4: Variation of Cu_2O sheet resistivity with sputtering pressure

Sputtering pressure ($x10^{-2}$ mbar)	**Sheet resistivity (Ω cm)**
1.8	33.6363
1.9	40.4532
2.0	53.9385
2.1	55.6848
2.2	56.3102
2.3	58.1463
2.4	62.2341

When the thin film sheet resistivities were plotted against the sputter pressures for the films, the graph below was obtained.

Fig. 5.5: Graph of Sheet Resistivity (Ω cm) of CU_2O thin films versus Sputtering Pressure (mbar)

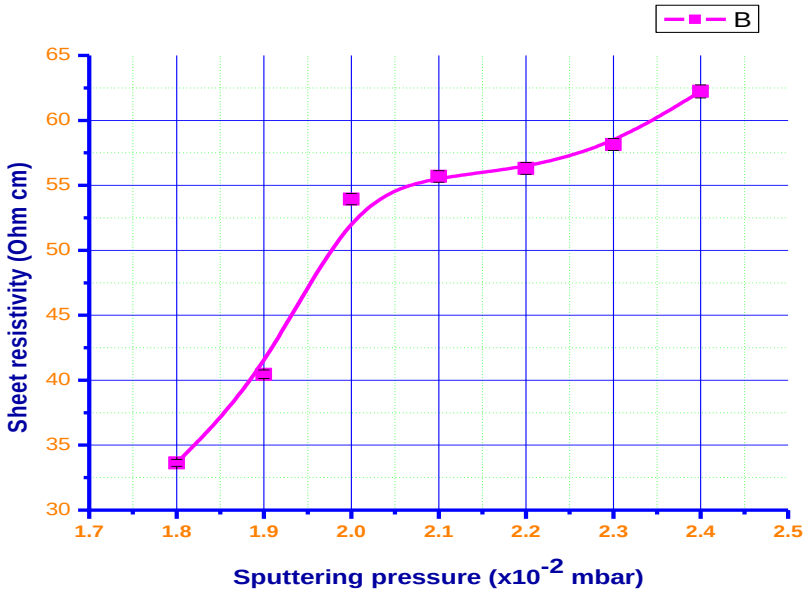

As depicted from the graph above, the sheet resistivities of the thin films increased from 33.6363 Ω cm to 62.2341 Ω cm with increase with sputtering pressure from $1.8x10^{-2}$ mbar to $2.4x10^{-2}$ mbar. The sputter pressure determines the mean free path, λ for the sputtered material. Together with the substrate-target distance, sputter pressure determines the number of collisions that occur on the particle's way to the substrate. This affects film porosity, texture and crystallinity. The low sheet resistivity at lower sputtering pressures may be attributed to high carrier mobility and carrier concentration since film's crytallinity is increased. The high sheet resistivity at higher sputtering pressures may be due to the amorphous nature of the films with the phases of Cu, Cu_2O and CuO present in the films. These results are in good agreements with the experimental results of Sivasankar *et al.*, 2007 in which sheet resistivity was found to increase with increase in sputtering pressure during the Cu_2O thin film deposition.

CHAPTER 6

CONCLUSIONS AND OUTLOOK

6.1 Conclusions

A simple, cheap, portable and computer-aided four point probe system required for sheet resistivity measurements has been designed and fabricated. A probe head and a Van der Pauw switching device have been fabricated. LabVIEW graphical software has been used to interface a SourceMeter 2400 and the switching device via a serial (RS-232) port and printer (LPT1) port, respectively. LabVIEW VIs have also been developed for data acquisition from the peripherals, data analysis and display by the computer. The software based system has been used to measure sheet resistivity of a test sample of DC sputtered cuprous oxide thin films both at room temperature and at different temperatures in order to prove the system's workability and reliability. At room temperature of 23 ^{o}C, the sheet resistivity was found to be 55.6548 Ω cm. As the temperature of the sample was raised from 23 ^{o}C to 170 ^{o}C, the film sheet resistivity decreased from 55.0837 Ω cm to 29.6691 Ω cm. The behavior of the measured sheet resistivity has been found to agree with the theoretical and experimental values with the decrease in sheet resistivity with rise in temperature being attributed to healing of crystal defects which could have arose during the thin film deposition (Sivasankar *et al.*, 2007). The sputtering pressure in the sputter coater during the thin film deposition has also been found to determine sheet resistivity of the thin films. As the sputtering pressure was increased from 1.8 x 10^{-2} mbar to 2.4 x 10^{-2} mbar, there was corresponding increase of sheet resistivity of the thin films from 33.6363 Ω cm to 62.2341Ω cm. Films formed at lower sputtering pressures had high crytallinity with high carrier mobility and carrier concentration while films formed at higher

sputtering pressures were more amorphous in nature with the phases of Cu, Cu_2O and CuO present in the films. This was attributed to a more porous films formed at high sputtering pressures (Sivasankar *et al.,* 2007). From the measurements of sheet resistivity of the test sample, films at varied temperatures and films prepared at different sputtering pressures, we can conclude that the designed and fabricated four point probe system offers a reliable solution for use in thin film sheet resistivity measurements.

6.2 Outlook

To improve on the accuracy of the sheet resistivity measured using the fabricated system, there is need to reduce contact resistance due to schottky effect between the probe tips and the sample's surface. Materials that do not introduce schottky barrier between their tips and the sample surface should be used. The results of these measurements can be improved by use of platinum rods for probe tips as opposed to aluminum tips that were used. Further studies should also be done using a tube furnace with an output port which can be interfaced to a computer for control and temperature measurements as the sheet resistivity is measured. This would help automate the system even further and improve the results. The same computer used for thin film thickness measurement by stylus-method profilometry should be used to control both the SMU and the switching device so that the computer and all the peripherals work in harmony as one unit. This would avoid thin film damage due to scratch. Sheet resistivity of thin films that are easily oxidized should be measured as soon as they are deposited to reduce the effects of deviations in the film's stoichiometry due to oxidation as this would severely affect the sheet resistivity measured (Ghosh *et al.,* 2000).

REFERENCES

Almen, O. and Bruce, G. (1961). Collection and Sputtering experiments with nobble gas ions. *Nuclear Instruments and Methods*. **11**(1): 257-278.

Balamurugan, B., Mehta, B.R. (2001). Optical and structural properties of nanocrystalline copper oxide thin films prepared by activated reactive evaporation. *Thin Film Laboratory*. **2**(14): 1-5.

Bautista, K. (2004). Thin film deposition, 2nd edition, University of Texas at Dallas, Erik Jonsson School of Engineering, USA, Pp. 67-120.

Bohdansky, J. (1984) A Universal relation for the sputtering yield of a monoatomic solids at normal incidence. *Japan Nuclear Inst. Met. Phys. Res. B.* **2**: 578-591.

Brown, M. and Jakeman, F. (1996). Theory of four point probe technique as applied to film layers on conducting substrates. *British Journal of applied Physics.* **17**: 1146-1149.

Ghosh, S., Avasthi, D., Shah, P., Ganesan, V., Gupta, A., Sarangi, D., Bhattacharya, R., Assmann, W. (2000). Deposition of thin films of different oxides of copper by RF reactive sputtering and their characterization. *Vacuum.* **57**: 377-385.

Gregor, T. G. (2007). Control and Measurement System for an Elevation over Azimuth Antenna Pedestal. *A dissertation submitted to the Department of Electrical Engineering, University of Cape Town, in fulfillment of the requirements for the degree of Bachelor of Science in Electrical Engineering,* South Africa.

Halperin, S. (1996). The difference between surface and surface resistivity. *Evaluation Engineering*. **35**(6): 49-50.

Higa, M.L.T., Lord, S.M. (2002). An Introduction to LabVIEW Exercise for an Electronic Class. *32nd Annual Frontiers in Education*. **1**: 6-9.

Jeffrey T. and Jim K. LabVIEW for everyone (2006), 3rd edition. Prentice Hall. Indiana, USA, Pp. 56-134.

Keithley 4200-SCS Inc. (2004). Four-Probe Resistivity and Hall Voltage Measurements with the Model 4200-SCS. *Application note series*. **2475**: 1-8.

Keithley Instruments. (1998). 2400 Series SourceMeter User's Manual. 2400S-900-01 Revision G. USA.

Maria, P., Gutierrez, S., Haiyong, I., Patton, J. (2002). Thin Film Surface resistivity. *In partial fulfillment of course requirements for Mate 210.* Experimental Methods in material Engineering, USA.

Markham, M. R. (1993). An interface for controlling external devices via the IBM PC/XT/AT parallel port. *Behaviour Research Methods, Instruments, & Computers*. **25**(4): 477-478.

Masato, Y., Toshifumi, N., Atsushi, I., Hiroshi, K., Nobuo, T. (1993). Resistivity correction factor for the four circular probe method. *Japan Journal of Applied Physics*. **32**(1): 246-25.

Matsunanmi, A., Yamamura, Y., Itikawa, Y., Itoh, N., Kazumata, Y., Miyagawa, S., Morita, K., Shimizu, R. (1980). A semiempirical formula for the energy dependenc of the sputtering yield. *Radiation Effects Letters.* **57**: 15-21.

National Instruments, (1998). National Instrument LabVIEW User manual, 320999D-01 Edition. USA.

Ogwu, A.A., Darma T.H., Bouquerel, E. (2007). Electrical Resistivity of Copper Oxide Thin Films Prepared by Reactive Magnetron Sputtering. *Journal of Achievements in Material and Manufacturing Engineering*. **24** (1): 1-6.

Ohring, M. (1992). The Material Science of thin films, Academic Press, United Kingdom, Pp. 34-79.

Onimisi, M.Y. (2008). Effect of annealing on the resistively of copper (I) oxide solar cells. *International Journal of Physical Sciences.* **3** (8): 194-196.

Owade, M.O. (1998). Design and development of a programmable interface system with illustrative use in resistivity-temperature experiment, *MSc. Thesis, Kenyatta University*. Kenya.

Pogula, S.S. (2005). Developing neural network applications using LabVIEW. *A Thesis presented to the faculty of the Graduate School, In Partial Fulfillment of the*

Requirements for the Degree of Master of Science. University of Missouri-Columbia. USA.

Reddy A.S., Rao, G. V., Uthanna, S., Reddy, P. S. (2005). Influence of substrate bias voltage on the properties of magnetron sputtered Cu_2O films. *Physica B.* **370** (9): 29–34.

Rick, B., Taqi, M., Matt, N. (2001). LabVIEW Advanced Programming Techniques. CRC Press, New York. USA, Pp. 24-74.

Schroeder, D. K. (1998). Semiconductor Material and Device Characterization, 2nd edition ,John Wiley and Sons, New York , USA, Pp. 217-342.

Sivasankar, R. A., Venkata, R. G., Uthanna, S., Sreedhara, R. P. (2007). Properties of dc magnetron sputtered Cu_2O films prepared at different sputtering pressures. *Applied Surface Science.* **253**: 5287–5292.

Sivasankar, R. A., Hyung-Ho, P., Sahadeva, R., Sarmab, K. U., Sreedhara, R. (2008). Effect of sputtering power on the physical properties of dc magnetron sputtered copper oxide thin films. *Materials Chemistry and Physics.* **110** (5): 397–401.

Smits, F.M. (1958). Measurement of sheet resistivity with the four point probes. *Bell System Technical Journal.* **37** (1): 711-718.

Sze, S. (1981). Physics of semiconductor devices. 2nd edition. John Willy & Sons, pp. 332-361. New York, USA, Pp. 56-67.

Toney, F., Walter, L., Emily, L., Wen-Y, L., Jonathan, D., Lawrence, C., Jonathan, H. (2003). *Applied Physics Letter.* **89**: 11-20.

Valdes, L. (1954). Resistivity Measurement of germanium for transistors. *Proc. IRE.* **42**: 420-427.

Van der Pauw, L.J. (1958). A method of measuring specific resistivity and Hall Effect of a disc of arbitrary shape. *Philips Technical Review. **20***: 220-224.

Wenner, F. (1916). A method of measuring Earth Resistivity. *Bulletin of the Burreau of Standard.* **12**: 469-4

APPENDICES

Appendix I: LabVIEW and its Features

LabVIEW is a graphical programming language developed in 1986 by National Instruments. It is a highly productive graphical programming environment that combines easy to use graphical developments with the flexibility of a powerful programming language. National Instruments LabVIEW is a revolutionary programming language that depicts program code graphically developed by simply connecting icons rather than textually.

Wires

Data transfer between block diagram objects is done through wires. Each wire has a single data source, but can be wired to many VIs and functions that read the data. Wires are of different colors, styles, and thicknesses depending on their data types. A broken wire appears as a dashed black line with a red X in the middle. The codes with broken data lines (Wires) cannot execute.

Structures

Structures are graphical representations of loops and case statements in text-based programming languages. They are used on the block diagram to repeat blocks of code and to execute code conditionally or in a specific order. The structures include for loop, while loop, sequential structure, timed loop, stacked sequence structure and formulae node.

Icons and Connector Panes

After building a VI front panel and block diagram, the icon and the connector pane are built so that this VI can be used as a sub-VI. Every VI displays an icon. An icon is a graphical representation of a VI. It can contain text, images, or a combination of both. If a VI is used as a sub-VI, the icon identifies the sub- VI on the block diagram of the VI. The icon can be double-clicked to customize or edit it. To use the VI as a sub-VI, a connector pane should be built. The connector pane is a set of terminals that correspond to the controls and indicators of that VI, similar to the parameter list of a function-call in text-based programming languages. Below diagrams shows examples of Icon and Connector Pane.

Icon - 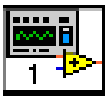

Connector Pane - 

Controls Palette

The controls palette is available only on the front panel. This palette contains the controls and indicators used to create the front panel. The controls and indicators are located on sub-palettes based on the types of controls and indicators. The figure below shows controls palette.

Functions Palette

The functions palette is available only on the block diagram. The palette contains the VIs and functions that can be used to build block diagram. The VIs and functions are located on sub-palettes based on the types of VIs and functions. The figure below shows a Functions Palette.

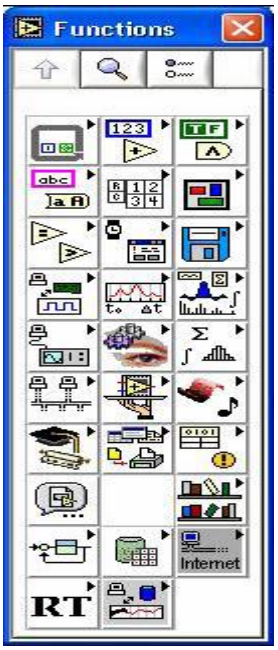

Tools Palette

The tools palette is available on the front panel and the block diagram. A tool is a special operating mode of the cursor. The cursor selects an icon corresponding to a tool in the palette. Tools can be used to operate and modify front panel and block diagram objects. The figure below shows a controls palette.

Indicators

Indicators are the interactive output terminals of the VIs. Indicators simulate instrument output devices and display data the block diagram acquires or generates. They include LEDs, graphs, charts and other displays.

Appendix II: Photograph of Stylus-method Profilometer

Appendix III: Photograph of Keithley SourceMeter 2400 model

Appendix IV: Photograph of the Designed and Fabricated Sheet Resistivity Measurement system